Experimental Investigation of the Response of Precast Segmental Columns Subjected to Impact Loading

Xihong Zhang*, Hong Hao and Chao Li

Centre for Infrastructural Monitoring and Protection, Department of Civil and Mechanical Engineering, Curtin University

Kent St., Bentley WA 6102, Australia

email: xihong.zhang@curtin.edu.au

Phone: +61 8 9266 9108

Abstract

Although precast concrete segmental columns have been more and more widely used in constructions, there is a lack of study on its behaviour under dynamic loading especially impact loading. In this paper, the fundamental behaviour of precast segmental columns under impact loading is investigated through laboratory tests. Scaled precast segmental columns with unbonded posttensioning tendon were constructed and tested by using pendulum impact system. Two segmental columns of the same height but with different numbers of precast segments were designed and tested. A conventional monolithic reinforced concrete (RC) column was also casted and tested as a reference column to compare the performance with segmental columns under impact loading. The impact load time history and column displacement time histories at column top, mid-height and column base were recorded. The deformation-to-failure processes of the columns were monitored by a high-speed camera, and used to investigate the response of different columns under impact loads. The test results showed the segmental column is more flexible than monolithic column, which leads to lower peak impact force but longer duration compared to those on the monolithic RC column. It was also found that comparing with monolithic column segmental column shows better performance against impact load with better self-centring capability, similar energy dissipation capability and less residual displacement and concrete damage.

1. Introduction

Recently much interest and attention have been directed to prefabricated structures, especially precast segmental structural members. This is mainly because precast structural elements can greatly reduce on-site construction time and cost, minimize traffic disruption due to construction work, improve work zone safety, reduce environmental impact, and improve construction quality. Time efficiency that can be achieved through utilizing precast segmental element is enormous. A study sponsored by the US Texas Department of Transportation (TxDOT) and the Federal Highway Administration (FHWA) concluded that using precast segmental element could reduce up to 50% construction time [1] (Figure 1a). Apart from the above advantages, new materials such as ultra-high performance concrete and fiber reinforced concrete, etc., which sometimes require heated curing and/or careful mixing,   can be easily applied in prefabrication factory to precast segmental elements.

Segmental columns have been popularly used in construction ever since ancient times. Many iconic structures around the world today were built hundreds or even thousands of years ago with segmental stone pillars, such as Brandenburg Gate, Germany built in 1788-1791 (Figure 1b), Tempo in Rhodes island, Greece built around 7th Century B.C. (Figure 1c). One of the earliest modern constructions that utilized precast segmental concrete elements was Lavaca Bay Causeway, Texas, US in 1961 [1]. The application of precast segmental columns has gained its popularity globally ever since. Numerous modern constructions have successfully used precast segmental concrete columns. Examples of buildings and bridge structures that employed segmental concrete columns can be found in reference [2, 3]. Despite all the above advantages, a major setback for precast segmental structures is that there is a lack of knowledge on its behaviour and performance under dynamic loadings, i.e. seismic loading, impact loading and blast loading.

2

So far most existing studies on segmental columns under dynamic loadings have focused on the evaluation and improvement of its seismic performance. Very limited studies are reported on the behaviour of segmental columns under impact and blast loading. Many studies have reported the response and failure mode of segmental columns under seismic loading. For instance, Ou et al. [5] carried out numerical and analytical studies. It was found that under cyclic loading segmental column exhibited flag-shape behaviour, and it could undergo larger drift than monolithic column. Shim et al. [6] performed laboratory test on scaled segmental columns. It was observed that the tested columns all exhibited flexural failure in the plastic hinge region near column base. Shear failure such as shear slip at segmental joints or concrete shear failure within segments was not found [7]. Under earthquake excitation the primary response modes of segmental column are mainly flexural. Friction force at the column joints is generally sufficient to transfer shear force. However, this observation may not be true for a segmental column under impact loading, where shear deformation may govern the response and damage of the column.

The influences of various column specifications, such as the number of segment/joint, prestress level, etc. have also been investigated in previous seismic analysis of segmental columns. For instance, ElGawady and Dawood [8, 9] performed experimental and numerical studies on unbonded circular segmental columns. It was found that before joint opened, large segment and small segment had the same shear stresses at a given drift angle; after joint opened, the smaller segment had higher shear stress. Shim et al. [6] also conducted scaled cyclic tests on a series of segmental columns. It was concluded that the number of segmental joints had no effect on the ductile behavior if the location of the segmental joint was far from the plastic hinge region. Therefore, it was recommended by Shim et al. that focus should be paid to the base connection between the segment and the footing in seismic analysis. For the effect of prestress level, Wang et al. [10] found that under seismic loading prestress tendon helped to reduce column residual displacement. Nikbakht et al. [11]

3

79   derived analytical solution and concluded that increasing prestress level would lead to

80   higher column stiffness, increased column strength and improved energy dissipation

81   capability. The influences of these factors on the performance of segmental column under

82   impact loading are not known.

83   As emphasized above, despite many studies on segmental column response under

84   seismic loading, research on impact resistance of segmental column is rare. The only article

85   available in the literature is a recent numerical study on segmental column under vehicle

86   impact [12]. A precast segmental column of 2.3m in diameter and 16.25m in height together

87   with a detailed truck was modelled in the analysis. Under the impact from the truck at

88   60km/h impact velocity, a slight lateral slip was observed at the base joint between the first

89   segment and the foundation. Therefore under lateral impact, shear resistance of the

90   segmental column could be a major issue. Comparison was made to the responses between

91   segmental column and cast-in-place monolithic column. A similar trend of concrete stress

92   was found on the segmental column and the monolithic column. Due to the relatively lower

93   stiffness, the response period of the segmental column was longer. Because of the large size

94   of the columns modelled, no apparent column damage or failure was observed in the study.

95   The failure of segmental column under impact load is therefore not investigated in that

96   paper. Till now, no experimental study or analytical solution of segmental column subjected

97   to impact loading can be found in the literature.

98   A few studies on the impact resistance performance of monolithic reinforced concrete

99   column have been previously carried out, which might provide some reference to the

100 possible response of segmental columns. Sha and Hao [13] performed experimental study

101 on monolithic RC pier under barge impact. Pendulum impact system was utilized in the tests.

102 Flexural failure was observed on the monolithic column at column mid-span where it was

103 impacted and also at column base. Numerical model of monolithic column under impact

104 loading was also built and validated with laboratory test results. Parametric study was

105 carried out to investigate the influence of column parameters such as column height,

106 diameter, and concrete strength, etc. on its responses. Some case studies on vehicle crash

107 resistance of monolithic RC column and steel column were previously reported. For example,

108 Buth and his co-workers [14, 15] performed experimental studies to evaluate the collision

109 loads on bridge piers. Silva et al. [16] also carried out experimental study to investigate the

110 impact resistance of RC column. El-Tawil et al. [17] evaluated the accuracy of AASHTO-LRFD

111 vehicle collision provision on RC column under vehicle impact through numerical analysis. All

112 these studies could help to predict the behaviour of segmental column under later impact

113 loading. However, since the response and failure mode of a segmental column could be very

114 different from that of a monolithic column, a proper study on segmental column under

115 impact loading is needed.

116 In this study, laboratory test was performed to investigate the response of segmental

117 column under impact loads using pendulum impact system. Two 800mm tall 100mm by

118 100mm squared segmental columns were casted. One column was designed with 5

119 segments and the other with 7 segments. A steel impacter weighting 300kg was lifted to

120 designated heights and then released to generate the impact loading on the mid-height of

121 the columns. A monolithic reinforced concrete column of the same height and cross-section

122 area was also tested as reference for evaluating the performance of segmental columns.

123 High-speed images of column deformation-to-failure process were recorded and used to

124 analyse column response. The impact load time history and column deformation were

125 recorded and analysed to evaluate the column performance.

126 **2. Test Setup**

127 To investigate the behaviour of segmental column under impact loading, three types of

128 scaled columns including two segmental columns and one monolithic reinforced concrete

129   column were designed and built in the laboratory. Pendulum impact system was utilized to

130   generate the impact loading onto the column. Details of the test specimens and the setup of

131   the pendulum impact system are described in the following.

132   2.1 Test specimens

133   Figure 2 shows the schematic view of the three specimens. The columns were 800mm in

134   height and had squared cross-sections of 100mm x 100mm in dimension. The designated

135   dimension of the tested columns represented quarter-scale model of a 3.2m tall residential

136   column. The height of the tested columns was restricted by the dimension of the pendulum

137   impact testing system for the current experiment. Previous studies by Woodson and Baylot

138   [18, 19] have demonstrated the suitability of quarter-scale model for RC column with similar

139   dimensions subjected to blast loading. Column damage and response including load and

140   deflection were well measured in their tests. It is therefore believed the current adopted

141   scaled model could be able to properly represent the behaviour of segmental column under

142   impact loading. A footing of 140mm deep and 400mm x 400mm cross-sectional area was

143   built for each column to bolt them onto the strong floor. The monolithic column was cast

144   with a 400mm x 400mm x 50mm flanges at its top to support the added mass. A concrete

145   block of 400mm x 400mm x 450mm (L x W x H) in dimension together with 5 pieces of 23kg

146   steel plates was placed on top of the columns, which gave a total weight of about 288kg on

147   top of the column. The weight of the column itself is about 18kg. The ratio of the supported

148   weight to the column self-weight was therefore about 16. Due to the restrain of the testing

149   system, there was no space for additional mass to be placed on top of the columns. Also,

150   because of the nature of impact test, inertia force from the added mass cannot be replaced

151   by directly applying axial force. No axial force was applied in addition to the added mass. The

152   barrels and wedges on both ends of the prestress tendons were anchored inside the footing

153   and on top of the steel plates.

154   Figure 3 depicts the details of the test specimens. For the monolithic column, 6mm

155   diameter longitudinal rebar was extended into the top flange and the bottom footing, which

156   created fully fixed boundary conditions for the monolithic column on both ends. The

157   segmental columns were connected to the footing using two 6mm diameter starter bars in

158   the direction of loading. No grout or epoxy was used to glue the base segment to the footing.

159   The top segment was left in direct contact with the concrete block above it. No

160   reinforcement or grout was used to connect the top segment and the concrete block. The

161   segmental column S5N included five pieces of 160mm tall reinforced concrete segments.

162   Four 4mm diameter ties at 40mm spacing were used to confine the concrete in each

163   segment. Column S7N comprised of seven segments of 115mm in height. 3 ties were

164   included in each segment. It is worth noting the previous studies on the seismic response of

165   segmental columns normally adopted columns with 2 to 6 segments [5-8]. Since plastic

166   hinge is normally formed near the column base, the number of segments has been found

167   having insignificant influence on column seismic response. For segmental column under

168   impact loading, number of segment in a column could influence the column performance,

169   because the impact may excite column local mode. Since this is the first impact test on

170   segmental columns, two types of columns with five and seven segments were prepared to

171   investigate the possible influence of the number of segments on its impact resistance. The

172   segment height to cross-section length ratio were 1.6 (160mm/100mm) for S5N and 1.15

173   (115mm/100mm) for S7N, which were similar to previously tested 4-segment and 6-segment

174   columns under cyclic loading. Since the columns were impacted at their centres, to avoid

175   impacting at segmental joints, columns with odd number of segments were designed and

176   tested. For the monolithic column, 4mm diameter ties were placed at 50mm equal spacing

177   throughout the column. For all the columns, 6mm diameter ribbed bars were used as

178   longitudinal reinforcement. For the segmental columns, the longitudinal rebar did not

179   continue between segments. Apart from the prestress tendon, there was no additional link

180   between adjacent segments. So under impact loading, the prestress tendon would take the

181   tensile force, and the joints of segmental columns were designed to open freely so as to

182   dissipate induced impact energy. Table 1 summarizes the specifications of the test

183   specimens. The monolithic column had a longitudinal reinforcement ratio of 1.14%, while

184   that of the segmental columns were slightly higher (1.16%) because of the void in the

185   centres of segments to allow for the prestress tendon. The bending and shear stiffness of

186   the monolithic column were about $2.65 \times 10^5 \text{N m}^2$ and $9.93 \times 10^7 \text{N}$. And its bending and shear

187   capacities were 2296N m and 22787N respectively.

188   For the segmental columns, a 15 mm diameter hole was left for the prestress tendon

189   when casting the columns. Seven-wire strands of 9.3 mm diameter were utilized as prestress

190   tendons. The properties of the tendon are listed in Table 2. A prestress load of 30kN was

191   jacked to the tendon after the columns were installed. The applied prestress load was about

192   10% axial capacity of the column. It should be noted that there is no guideline yet on the

193   level of prestress for segmental column. The applied prestress load resulted in about

194   400MPa stress in the tendon, which is much lower than material yield stress. This

195   application ensured the tendon would not yield when the column deforms, and would

196   provide sufficient restoring force to pull the column back to its original position.

197   2.2 Fabrication and material properties

198   For quality control of the scaled column specimens, much attention was paid to the

199   fabrication of formworks (Figure 4). Careful alignment was ensured during the fabrication

200   and pouring of concrete to minimize construction errors. It was also important to ensure the

201   position of reinforcement and the concrete cover depth.

202   Grade 25 self-compacting concrete with super plaster was used for casting of concrete

203   columns. The maximum aggregate size was 10mm. The average compressive strength (fc') of

204 concrete from five quasi-static compression tests on 100mm diameter by 200mm height

205 cylinders under standard curing condition was 34 MPa. The flexural tensile strength (f_t) of

206 concrete from three four-point bending tests on 600mm x 100mm x 100mm (L x D x W)

207 specimens was 5 MPa. Table 2 summarizes the material properties of concrete,

208 reinforcement and prestress tendon.

209 2.3 Instrument setup and measurement system

210 Pendulum impact system was utilized in the current test. The pendulum impact system

211 consisted of a steel frame, a pendulum arm, an impactor, and an inclinometer. As shown in

212 Figure 5, the steel frame was fixed on the strong floor to support the entire test system. A

213 300kg steel impactor was connected to the frame through a 2.8m long pendulum arm. In

214 each test, the impactor could be lifted to a desired height (quantified through the lifting

215 angle) and then released to strike the mid-height of the column. After the impactor hit the

216 column and rebounded, the impactor was pulled back immediately to avoid a second impact

217 on the column.

218 Figure 6 illustrates the measurement system. To measure the applied impact load a 25t

219 load cell was fixed in front of the impactor. The load cell was calibrated on Baldwin universal

220 testing machine. Three laser Linear Voltage Displacement Transducers (LVDT made by

221 Keyence) were placed at column mid-height, column top and near column base behind the

222 test specimens. The LVDT has a measuring range –of 150 mm each direction. The sensors

223 were wired to a NI USB-9237 acquisition system and the data were captured at a sampling

224 frequency of 50 kHz. A high-speed camera (Photron SA-Z) was installed to monitor the

225 deformation-to-failure process of the columns. The filming rate of the high-speed camera

226 was set to 8000fps. The exposure time was set to balance with the aperture. Four halogen

227 lights were used to provide intensive light for high-speed filming. Five tracking dots were

228 glued to the middle of each segment for the segmental column S5N on its side. Another

229 group of five dots were glued to the same heights on the monolithic column. And similarly

230 seven tracking dots were used for column S7N. The high-speed camera images were post-

231 processed using digital image correlation software to derive the column displacement time

232 histories at these tracking dots. For easy interpreting the test results, the segments and

233 joints are numbered as Segment 01-07 and Joint 01-08 respectively (as depicted in Figure 3).

234 **3. Test Results**

235 The columns were tested with multiple impacts with progressively increasing the impact

236 speed. The release angles of impactors started from 2.5 degree (Impact 01) which

237 corresponded to an impact velocity of about 0.23 m/s. Then, the release angles were

238 increased to 7 degree (Impact 02), 15 degree (Impact 03), and 30 degree (Impact 04), which

239 corresponded to impact velocities of 0.64 m/s, 1.37 m/s and 2.71 m/s, respectively. After

240 the above four impacts, if the column was still standing and holding the added mass, a final

241 impact with release angle of 40 degree (Impact 05) and impact velocity of 3.58 m/s was

242 carried out which resulted in a thorough failure of the column. The initiative of the designed

243 impact velocity was to assess the elastic response, minor damage, medium damage and

244 ultimate failure of the columns under impact loading. Detailed observations on the test

245 columns including high-speed camera images, column damage and failure modes are shown

246 below. Quantitative results such as impact load time history, column displacement time

247 history and displacement contours were also presented in the following section.

248 3.1 Qualitative results

249 3.1.1 Deformation-to-failure process

250   The response of each column under the strike of the impactor was monitored by a high-

251 speed camera. Figure 8 and Figure 9 show the deformation-to-failure processes of the

252 columns under progressively increased impact loading. Since the impact loads were

253 relatively small in Impact 01 and 02 none of the columns experienced any significant

254   deformation, the high-speed camera image sequences for Impact 01 and 02 are therefore

255   not presented here. However, using digital image correlation the high-speed camera images

256   were post-processed to derive the lateral displacement histories at the tracking dots. Then,

257   the lateral displacement contours of these columns were mapped and presented for better

258   illustration of the responses of the columns (Figure 7 and Figure 10).

259   As shown in Figure 7, in Impact 01 and 02 when the impact forces were relatively small

260   the monolithic column deformation shape followed the local element mode with the large

261   displacement initially occurred at the impacted location. This is because of the large inertial

262   resistance generated by the lumped mass at the top of the column specimen upon impact,

263   which prevented large movement of the column top although it was not restrained. The

264   deflection shape, however, quickly changed to the fundamental mode of the column,

265   especially in the free-vibration phase (the impact loading duration is about 0.02 to 0.03 sec

266   as shown in Figure 12) with the largest displacement at the column top. This is expected as

267   the column requires least energy to vibrate with its fundamental mode. It could be observed

268   that only positive deflections were developed on the monolithic column. In Impact 01,

269   because the impact velocity was quite small, less noticeable inertia resistance was

270   developed at the lumped mass on column top as compared to that in Impact 02. After

271   Impact 02, concrete cracks were observed in the rear surface of the central part of the

272   monolithic column indicating flexural tensile failure in the concrete. A diagonal shear crack

273   was also found near the column base (Figure 11b). As shown in Figure 8a, when the

274   monolithic column was impacted by the impactor released at 15 degree in Impact 03, the

275   existing cracks around the mid-height of the column extended and opened further under the

276   action of the lateral impact (t=5ms). The column showed an apparent large central

277   deflection (t=26ms) indicating flexural deformation. A peak deflection of 14.6 mm was

278   measured at the centre of the column. The shear crack near the column base was also

279   widened under the impact loading (Figure 11a). Catastrophic column failure was resulted in

280 Impact 04. As shown in Figure 9a, upon the impactor struck onto the column the existing

281 cracks around the mid-span opened and began to extend at t=0.4ms. As the impactor forced

282 the damaged column to further deform laterally, flexural cracks grew into major cracks and

283 quickly extended across the central part of the column, and concrete crush occurred on the

284 other side of the column (t=4ms). The significant lateral impact loading also widened the

285 existing shear crack near the column base. A complete concrete shear failure occurred at

286 t=7ms, and the shear force was merely resisted by the reinforcement. A total column

287 collapse was observed at t=57ms with a flexural bending failure at the centre and base of

288 the column and also a thorough diagonal shear failure near the base of the column.

289 The segmental column responded very differently to the impact loading. As depicted in

290 the contour in Figure 7a, under the low level impact force in Impact 01, upon the impact the

291 centre of the segmental column S5N deformed faster than column top and bottom. A peak

292 deflection of 3.9 mm was reached at the centre of the column at t=20ms. This is because of

293 the inertia resistance from the added mass on column top, which restrained the lateral

294 displacement of the column top. After reaching the first peak deflection at column centre,

295 the central part of the column rebounded under the action of the prestress tendon. In the

296 meanwhile, the top part of the column continued to deform sideways with its lateral

297 displacement exceeded that in the centre of the column. The entire column vibrated freely

298 around its original position until it came to a rest. Similar response was observed for column

299 S5N in Impact 02. No apparent damage was found on this segmental column after Impact 02.

300 When the impactor was released at 15 degree, damage to the segmental column appeared.

301 As shown in Figure 8b, at t=5ms, as the flexural induced compressive stress in the concrete

302 exceeded its compressive strength, concrete crack was formed on the top left corner of

303 Segment 03. As the impactor forced the column to further deform and bend, the concrete

304 crack extended. At t=45ms, the top left corner of the segment failed due to compression. An

305 apparent joint opening was found between the Segment 03 and 04. The joint opening

12

developed wider as column S5N continued to deform and bend. But the size of opening

gradually reduced and then closed as the deformation shape transformed from a mid-span

deformation governed flexural bending to top deformation led free-vibration (shown in

Figure 8b). The entire column vibrated freely around its base. A maximum displacement of

around 53 mm was measured at the top of the column. The large bending force transferred

through the column and starter bars to the footing, which resulted in minor damage to the

footing (t=252ms). Nevertheless, the segmental column S5N eventually restored to its

original position with a small residual displacement (δ_{resi}=3.8mm) at column top. In Impact

04, larger joint opening was found as a result of more significant flexural bending under the

increased impact loading. Concrete in the compressive surface of this joint was further

crushed because of the flexural compression and also the direct impact force on the

segment. In the meanwhile, because of the excessive flexural bending the base segment

(Segment 01) was bent and rotated with its right bottom corner crushed against the footing

(t=78ms in Figure 9b). Owing to the rotation of the bottom segment, the starter bar pulled

the footing, which resulted in some tensile damage to the concrete footing. Nevertheless,

the segmental column still supported the added mass on its top. Because the footing was

damaged no further test was carried out.

The response of column S7N was very similar to column S5N especially in Impact 01 and

02 when the levels of impact load were low. When the impact load was increased with the

impactor released at 15 degree, concrete compressive failure was also observed. But as

shown in Figure 8c, the segmental column bent in the centre at t=13ms as the impact

excited the local mode of the column. As the column continued to deform, the curvature

began to shift upwards, and the local mode gradually transferred into global mode with the

largest curvature shifted from column centre towards column top. At t=37ms, with excessive

lateral deformation compressive stress in the concrete at the Segment 05 and 06 reached

failure stress. Concrete was crushed in the compressive face of the two segments. With the

13

332 further increased impact load by releasing the impactor at 30 degree (Figure 9c), the centre

333 of the column was forced by the impactor to bend significantly. More severe concrete

334 crushing failure occurred on Segment 04 and 05 at t=120ms because of the large flexural

335 induced compressive failure and also the large impact force from the impactor directly.

336 Some compressive damage on the base segment (Segment 01) was also found as the column

337 rotated against its base. An opening could be observed in the base joint (Joint 01) as the

338 column experienced large flexural bending. Despite the damage to concrete in some

339 segments, after free vibration column S7N still managed to survive the impact with obvious

340 residual deformation. A final impact (Impact 05) was then carried out on column S7N to

341 examine its ultimate impact resistance capability. Figure 9d shows the deformation-to-

342 failure process of the column. As can be seen, Segment 04 in the middle of the column was

343 badly smashed by the impactor. As the column bent, Segment 05 was seriously crushed due

344 to the extreme flexural bending. The base segment was also severely damaged in its

345 compressive surface as it rotated around the footing (Figure 11). Plastic deformation was

346 formed in the starter bar, and after Impact 05 column S7N was left with large residual

347 deformation. Because the compressive damage extended to the neutral axis in Segment 05,

348 the segments and the added mass above Joint 05 lost its stability and the column was

349 considered failed completely.

350 3.1.2 Failure mode

351 The failure of the monolithic column was governed by flexural failure and shear failure.

352 As the level of impact load increased, flexural tensile damage to concrete in the rear face of

353 the monolithic column was observed in Impact 02 (Figure 11b), which grew into major

354 critical cracks (Figure 11a). The tensile cracks led to the flexural failure of the column (Figure

355 11d) when the impact load was further increased. Diagonal shear failure near column base

356 was also found in the monolithic column which also initiated in Impact 02 (Figure 11b). As

14

357 the impact loading was increased, the shear crack further developed leading to complete

358 failure of the column.

359   The damage and failure pattern of the segmental columns differed from those of the

360 monolithic column. Under the lateral impact loads, the columns also exhibited flexural

361 deformation. Instead of resulting in concrete tensile cracks, segmental joints opened in

362 responding to larger curvature in the column. When the column was subjected to larger

363 impact loading, compressive damage to concrete in the compressive side of the joint would

364 be expected (Figure 11c). When the segmental columns were subjected to large flexural

365 deformation, the base segment rotated at the footing. Compressive damage to base

366 segments occurred when the compressive stress exceeded the concrete strength (Figure 11d

367 and c). Also, the footing around column base would be subjected to larger flexural actions. If

368 no starter bars were used, the prestress tendon would take the tensile force and the

369 concrete segment take the compressive force. When starter bars were used to connect the

370 base segment and the footing, which was quite commonly adopted in seismic design so as to

371 improve energy dissipation capability, the force transferred to the footing would increase.

372 Damage to footing was therefore more likely to occur (Figure 11d).

373 3.2 Quantitative results

374   The impact load time history, displacement time histories at column top, centre and base

375 were recorded during the tests. Because the restrain of footing, the displacement at column

376 base was generally quite small except for the monolithic column with shear failure.

377 Therefore, the displacement at column base is not given here. The test results including the

378 peak impact force, maximum column central displacement and residual displacement, and

379 the maximum and residual displacement at column top are summarized in Table 3 and 4.

380 3.2.1 Impact load time history

381   The impact load is an important parameter for analysis of column impact resistance

382   performance. Figure 12 shows the load time history measured on the columns. As shown in

383   Figure 12a, in Impact 01 upon the impactor stuck on the monolithic column the load

384   increased sharply to about 12kN then attenuated gradually to zero. The sharp rise in the

385   impact load was because of the rigid impactor itself, the stiffness and inertia resistance of

386   the column. As the release angle was increased to 7.5 degree and 15 degree, the peak

387   impact load rose to about 22kN and 38kN, respectively. The loading duration also became

388   slightly longer (30ms and 45ms). In Impact 04, the peak impact load reduced to about 29kN

389   because the monolithic column was severely damaged in the previous impacts and lost

390   much of its stiffness. The shape of the impact load on the monolithic column was primarily

391   triangle shape which differed from the five-point impact loading diagram to model the

392   vehicle impact loading [12]. This is because the impactor in the current pendulum impact

393   system was made of solid steel blocks, which was much more rigid than that of the vehicle in

394   the reference. The latter will deform significantly as the vehicle impacts on the column

395   which leads to a more gradual rising phase of the load.

396   The impact load time histories recorded on the segmental columns were different from

397   those on the monolithic column. Figure 12b shows the load time histories for the segmental

398   column S5N. As shown, upon Impact 01 the load quickly increased to about 7kN when the

399   impactor stuck on the column. The load reduced gradually after the peak force to about

400   2.5kN. Then it increased to about 7kN resulting in a second peak load. The two-peak impact

401   load time history on the segmental column differed from that on monolithic column which

402   had only single peak. There are two possible reasons: firstly, this is because of the

403   interaction between the impactor and the segmental column. As shown in Figure 13b, the

404   LVDT behind the centre of the column monitored that the central segment quickly reached a

405   peak displacement under the impact force. It then rebounded quickly back. This response of

406   the central segment in contact with the impactor resulted in the 2nd peak load on the load

time history. Secondly, the second peak could be resulted from the prestress tendon. The 9.3mm diameter tendon was placed in the 15mm hole of the segments. There was in general a gap of 2-3mm between the segment and the prestress tendon. When the impactor struck on the column, only the concrete segments provided resistance. But as the impactor forced the segments to deflect and hit the post-tensioned tendon, the tendon also provided resistance to the impactor. Hence another peak on load time history was formed. In future test, the force in the tendon shall be monitored to validate this explanation. As the impactor were released at larger angles, i.e. 7.5 degree and 15 degree in Impact 02 and 03, the peak loads increased to about 13.5kN and 21kN. Because the central segment was damaged in Impact 03 and 04, the interaction between the load cell and the column became more complex as evidenced on the tracked load time histories which were associated with more fluctuations. Since the column was damaged with degraded stiffness, the peak impact load measured on Impact 04 was merely above 22kN but with longer duration (about 180ms). Similar load time histories were recorded on column S7N. In Impact 03, since segment damage was only found on Segment 05 and 06 whereas the central segment (Segment 04) was still intact, no load fluctuation was observed during its attenuation phase. Instead, fluctuation was found on load time history in Impact 04 and 05 when the central segment experienced significant damage. As the column suffered severe damage in Impact 04, the peak load measured in Impact 05 reduced to about 20kN whereas a peak of about 24kN was measured in Impact 04.

The recorded load time histories were integrated with time to derive the corresponding impulses. Together with the peak impact forces, the derived impulses are provided in Table 3. The measured impact load time histories for the three tested columns at each impact velocities showed consistency. It is therefore believed that the measured load time history is reliable. The impact velocity was estimated from the releasing height of the impactor as well as the high-speed camera images. It is to note that for conservation of momentum the

433 impulse is related to not only the initial velocity and rebound velocity of the impactor but

434 also the momentum, deformation and damage of the column. Since the impact energy

435 would impart into the column and consumed by converting to the column kinetic energy,

436 elastic and plastic energy, and by friction between segments and segments opening and

437 closing, etc., it would not be accurate enough to only assess impactor initial and rebound

438 velocities to check the consistency of impulse.

439 3.2.2 Central and top displacement time histories

440   The lateral displacements were measured by the LVDT, which were carefully validated

441 with the measurements of high-speed camera images before being analysed. The column

442 central and top displacement time histories are plotted in Figure 13. For the monolithic

443 column, peak central deflections of about 5.2 mm and 7.5 mm were resulted in Impact 01

444 and 02, respectively. In Impact 03, a peak central deflection of about 14.6 mm was

445 measured. In Impact 04, because the monolithic column failed directly under the significant

446 impact force, the recorded central deflection increased sharply to over 200 mm (Figure 13a).

447 The central deflections of the segmental columns were very different from that of

448 monolithic column. In general, the maximum deflections at column centres were found

449 during the forced vibration phase. The columns rebounded and then further deflected to

450 reach a second peak deflection. The measured peak central deflections increased under

451 larger impact load. For the segmental column S5N, in Impact 01 a peak deflection of 3.9 mm

452 was measured, while the peak deflections increased to 7.7 mm and 32.8 mm when the

453 impactor was released at 7.5 degree and 15 degree in Impact 02 and 03, respectively. In

454 Impact 04, the peak deflection rose to about 108.4mm despite the measured impact load

455 did not increase substantially. This larger deflection recorded was mainly because of the

456 degraded column stiffness in the previous impacts and also the longer loading duration in

457 this impact. The peak central deflections measured on the segmental column S7N were

458 slightly larger than those in column S5N. A maximum central displacement of 5.1 mm and

459   11.5 mm were found for column S7N in Impact 01 and 02. This was mainly because the

460   segmental column S7N with more segments was relatively more flexible than column S5N. In

461   the following impact, peak deflections of about 24 mm and 104 mm were measured on

462   column S7N in Impact 03 and 04.

463   The lateral displacement at column top strongly influences the performance of the

464   column. Because of P-delta effect, large lateral displacement at column top would introduce

465   large moment to the column and increase the potential of column overturn and collapse.

466   Figure 13b shows the recorded displacement time histories at column top. For the

467   monolithic column, the peak displacements at column top were in general larger than that

468   at the centre of the column. For instance, in Impact 01 and 02 the column top displacements

469   of 6.6 mm and 11.7 mm were recorded, whereas those at column centre were 5.2 mm and

470   7.5 mm. For the segmental columns, peak column top displacements occurred during free

471   vibration phase after the impact, and the values were normally larger than those at column

472   centres. For example, in Impact 01 when the impact load was small a maximum column top

473   displacement of about 6.1 mm were found on S5N, while the maximum displacement at

474   column centre was 3.9 mm. In Impact 04 when the impact load was large, a maximum top

475   displacement of 116 mm was recorded while the maximum displacement at column centre

476   was about 108 mm.

477   3.2.3 Residual displacement

478   Residual displacement of columns after the impacts was another concern. The residual

479   displacements on the tested columns at each impact velocity were measured by LVDT.

480   Considering the large amount of data, some of the displacement time histories were

481   abridged so as to concentrate on comparing column forced response. As shown in Figure 13,

482   after the impact loading the monolithic column vibrated freely but because of plastic

483   deformation of reinforcement and concrete damage, the monolithic column would not

19

484   restore its original position. A residual displacement of about 1.5mm was recorded at the

485   column centre after Impact 01. Increased permanent deformation was accumulated in the

486   impacts with residual displacements of 3.0 mm and 11 mm at column centre after Impact 02

487   and 03. In comparison, the segmental columns exhibited much better self-centring capability.

488   Under the low level impact forces, the segmental columns deformed and then vibrated

489   freely. They were always capable of coming to their original positions with very small

490   residual displacements. For example, after Impact 01 and 02 the residual displacements at

491   the centre of column S5N were merely 0.5 mm and 1 mm respectively. Those for column

492   S7N with more segments were slightly larger (0.7 mm for Impact 01 and 1.6 mm for Impact

493   02). Even under large level impact loads when damage occurred to concrete, a significant

494   less residual displacement was observed by the segmental columns. For instance, after

495   Impact 03 the residual central displacement of column S5N was 3.6 mm and that for column

496   S7N was only 2.6 mm. After Impact 04 in which concrete segments experienced partial

497   compressive damage, the residual displacement at the centre of column S7N was slightly

498   over 7 mm. Therefore, it can be found comparing with conventional monolithic column

499   segmental column shows much better self-centring capacity when subjected to lateral

500   impact loading. The better self-centring feature of segmental column was primarily because

501   of the following two reasons: firstly, when the segmental column deformed sideway, the

502   horizontal component of the large prestress force in the tendon would pull the swayed

503   column back to its original position. Secondly, since the longitudinal reinforcements in the

504   segments do not extend through the entire column, the flexural deformation of the column

505   under lateral loading mainly led to the opening and closure of segmental joints. No plastic

506   deformation was developed in the reinforcements. The flexural tension within the cross

507   section of the segmental column was undertaken by the prestress tendon. With much higher

508   yield strength of material and proper designed tendon diameter, much less or even no

509   plastic deformation could be developed in the prestress tendon.

4. Analysis and discussion

In this section, the performance of segmental column under lateral impact loading is analysed. Comparison is made between segmental column and conventional monolithic column. Analysis is made with regard to the impact load, lateral displacement at column centre, and energy dissipation. The effect of the number of segments is also discussed.

4.1 Impact load

The impact load onto the column is an important factor when studying column impact resistance capability. As described in Section 3, despite the impactor was made of the same weight and was released at the same height each time, the measured impact loads varied between the two segmental columns and the monolithic column. This was mainly because the action of the impactor was coupled with the response of the target column. To better analyse the impact load and the response of the segmental column, the measured load time histories for the three different columns in each impact are summarized and plotted together in Figure 14. As shown in Figure 14a for Impact 01, the load on the monolithic column increased more sharply as the impactor struck on the column, while because of the relatively low stiffness with segmental joints, the loads on the two segmental columns increased more gradually. A peak load of about 12kN was measured on the monolithic column while those for the segmental columns were around or below 8kN. 38% and 31% lower peak loads were resulted on segmental columns S5N and S7N respectively. After reaching the peak load, the impact force on the monolithic column dropped quickly to zero. The total loading duration on the monolithic column was only about 20ms. Because of the deformation and rebound of the segmental column, the impact forces made second peaks after they reduced from the first peak loads. It should be noted that from mechanical point of view, a segmental column can be simplified as a series of bars jointed by non-linear springs. Column S5N and S7N were of the same height and cross-section. And the moment-

535   curvature relation for the joint spring would also be the same as the same level of prestress

536   was used. Column S7N comprised of more joints than S5N. Under the same loading, more

537   joints would open on S7N than S5N, which results in larger deflection. Therefore, S7N is less

538   stiff than S5N. As a result, the loading duration on S7N was slightly longer (approximately

539   52ms) than column S5N (about 42ms). Similar impulses were found on segmental column

540   S5N (141kN ms) and monolithic column (134kN ms); while due to longer loading duration

541   larger impulse was resulted on column S7N (about 203kN ms). Similar trend can be observed

542   in Figure 14b for Impact 02. With the impactor released at 7 degree, the peak impact force

543   on the monolithic column increased to about 22kN, while those on the two segmental

544   columns S5N and S7N were about 13kNand 12kN which were 38% and 45% less than that on

545   the monolithic column.   And the loading durations extended to about 30ms for the

546   monolithic column, which was still shorter than those on the two segmental columns (50ms

547   for S5N and 66ms for S7N). The impulse on column S5N (300kN ms) was still approximately

548   the same with monolithic column (290kN ms), while that on column S7N was about 10%

549   (323kN ms) more than that on monolithic column. Despite the monolithic column suffered

550   damage (concrete tensile cracks and diagonal shear crack) in the previous impact, the peak

551   impact loading on this column in Impact 03 was still much higher than the two segmental

552   columns. A peak load of about 38kN was recorded. Much lower peak forces were recorded

553   on the two segmental columns. The peak load measured on column S5N was slightly larger

554   (about 21kN, but 45% less comparing with the monolithic column) than that on S7N (about

555   17kN, and 57% less comparing with the monolithic column). This was because with more

556   segmental joints, S7N is more flexible than S5N. In the meanwhile, as the loading duration

557   on the segmental columns was longer, 15% and 17% higher, impulses resulted on column

558   S5N and S7N were larger than that on the monolithic column. Upon the impact, column S7N

559   exhibited more joint openings. In Impact 04, the peak impact force on the monolithic

560   column dropped to about 29kN as the column was previously damaged. The impactor forced

22

561 the column to deform to failure and the loading duration was merely about 30ms. Despite

562 both of the two segmental columns experienced minor concrete crushing damage in their

563 segments, in face of the impactor striking with higher velocity they were still capable of

564 resisting the impact. Larger peak impact forces were measured on these two columns than

565 previously in Impact 03. As shown in Figure 14d, for column S5N the impactor forced the

566 column to deform. After reaching a peak load of 22kN, the force reduced quickly to almost

567 zero because the concrete bearing the impacting force was crushed. As the impactor

568 continued to push the column forward, the force increased and then dissipated gradually.

569 The recorded peak forces and the derived impulses are summarized and plotted in Figure

570 15. As shown, when the impactor of the same weight struck with the same impact velocity

571 (same releasing angle), higher peak forces were always observed on the monolithic column

572 than that on the segmental columns. But similar or even larger impulses were always found

573 on the segmental columns because of longer impact duration. The peak forces on the

574 segmental column with five segments were slightly higher than that on the one with seven

575 segments. This is because the stiffness of column S5N was relatively higher than that of

576 column S7N with more joints.

577 4.2 Column response

578 To evaluate column response under impact loading, the recorded central deflection time

579 histories in each impact test are plotted and compared in Figure 16. Under the impact

580 loading, the responses of the monolithic column were featured with a peak deflection and

581 the column quickly rebounded with noticeable residual displacements. The behaviour of the

582 segmental columns was very different. A peak central deflection was usually resulted during

583 the forced vibration phase. The columns then rebounded but quickly vibrated back to make

584 a second peak deflection. The segmental columns then vibrated freely about their original

585 positions until they came to a rest, with much smaller residual deflections. In addition, the

23

586 segmental column with more joints vibrated slower than the other one with less number of

587 joints. For instance, in Impact 01 the free vibration period of column S5N was about 0.4s,

588 while that for column S7N was nearly 0.6s. It indicates column S5N is stiffer than S7N. It is

589 worth noting that in Impact 01 and 02, there was no apparent joint opening observed

590 through the high-speed camera images as shown in Section 3. With the same column

591 dimension, reinforcement ratio, prestress force, and boundary condition, the stiffness of the

592 segmental columns with different number of joints still differs. The test results therefore

593 show that even before any joint opening is formed, it is not appropriate to simplify the

594 segmental column with Bernoulli-Euler beam theory when estimating its deflection.

595 When segmental joints opened, the period of the column became longer. As shown in

596 Figure 16c, when the joint of column S5N was forced to open in Impact 03 the vibration

597 period stretched to 0.7s. But as column rebounded the opened joint was closed. It is

598 evidenced that the deflection curve was not a smooth sinusoidal curve. With multiple joint

599 openings on column S7N, the vibration period was even longer.

600 To evaluate the response of the segmental columns and compare their performance with

601 monolithic column, the maximum column central deflections are summarized and plotted

602 versus the impulse that each column experienced. As shown in Figure 17a, in general the

603 maximum deflection increases with the applied impulse for both monolithic and segmental

604 columns. When the impulse was low, a larger maximum deflection was found on the

605 monolithic column than on the segmental columns. For instance, when the impulse was

606 about 128kN ms, a maximum deflection of 5.2 mm was measured on the monolithic column

607 while under a similar impulse, the maximum deflection of the segmental column S5N was

608 3.0mm (42% less than the monolithic column). Although the impulse was much larger on

609 column S7N (about 192kN ms), the measured maximum deflection was still smaller (5.1mm).

610 This was mainly because the prestress prevented joint opening on the segmental columns

24

when the impact load was relatively small, which minimized the column deflection. As the

impulse increased, joint openings occurred. Larger maximum central deflections were then

measured on segmental columns than those on the monolithic column. For example, a

maximum central deflection of 14.6mm was measured on the monolithic column when

subjected to 478kN ms impulse. In comparison, the maximum deflections of 32.8mm and

24.3mm were recorded on column S5N and S7N with respect to about 560kN ms impulse.

Under approximately the same impulse in Impact 03 and 04 the maximum deflections of

column S5N were 26% larger than those of S7N. This was because the footing of column S5N

was partially damaged which led to a more flexible base connection for this column in

Impact 03 and 04.

The segmental columns show more advantages over monolithic column in terms of

residual deflection. As shown in Figure 17b, for all the impacts in the current study smaller

residual deflections were always measured on the segmental columns. For instance, under

low level impulse (approx. 128kN ms and 288kN ms for Impact 01 and 02), residual

deflections of 1.5mm and 2.9mm were measured on the monolithic column. In comparison,

less than 1mm residual deflections (merely 1/3 of that on monolithic column) were

measured on the segmental column S5N. As the impulse increased to about 480kN ms, the

monolithic column experienced severe flexural and shear damage with a residual deflection

of about 11 mm. In contrast, under even larger impulse (about 560kN ms), a residual

deflection of 3.6mm was found on the segmental column S5N, which was over 67% less than

that on monolithic column. It can therefore be concluded that under lateral impact loading

segmental column shows much better self-centring capacity than conventional monolithic

column. This was because no plastic deformation was formed in its longitudinal

reinforcement and the prestress tendon inside the segmental column pulled the swayed

column back. It should be noted that the level of residual displacement should also depend

on the prestress level, which will be investigated in future studies. Similar level of residual

637 deflections was found on the two segmental columns S5N and S7N under low level impact

638 loading because there was no joint opening on either column. When column S5N was

639 subjected to about 144kN ms and 288kN ms impulse, the residual deflections were about

640 0.5mm and 1mm. Under about 208kN ms and 320kN ms impulse, the residual deflections of

641 column S7N were 0.7mm and 1.6mm (indicating 40% and 60% more than those of column

642 S5N), respectively. Again, because the footing of column S5N was damaged in Impact 03, the

643 footing could not provide the same restrain to the column. As a result, larger residual

644 deflections (about 3.6mm and 28.0 mm) were measured on column S5N when subjected to

645 560kN ms and 912kN ms impacts. Under the similar magnitudes of impulses the residual

646 deflections of column S7N were 2.6 mm and 7.3 mm, respectively.

647 4.3 Energy absorption

648 Energy absorption is another important parameter in evaluating column impact

649 resistance capability. The energy absorption depends on the load and deformation history

650 rather than the permanent deformation. Figure 18 shows the impact load versus column

651 central deflection for the three columns in each impact. The enclosed area by the load and

652 deflection curve represents the energy dissipated through column deformation and damage.

653 According to Figure 18, the impact loads on the monolithic column are in general higher

654 than those on the segmental columns. But the deformations of the segmental columns are

655 always larger. It is therefore not straightforward to directly assess the energy dissipation

656 capabilities of the columns. The dissipated energy derived from the enclosed area of the

657 load-deflection curves are plotted against the impulses. As shown in Figure 19 when the

658 applied impulses were relatively low, very similar levels of the energy were dissipated by the

659 monolithic column and the segmental column. The monolithic column failed at the impact

660 with an impulse of about 480kN ms, but the two segmental columns were still capable of

661 resisting impact loads and dissipating more energy. The monolithic column dissipated the

662 impact energy mainly through plastic deformation of reinforcement and damage of concrete.

663 Damage accumulated with noticeable residual displacement even under small impact.

664 Segmental column was capable of dissipating the imposed impact energy through more

665 versatile forms. Upon impact, the column could deform substantially owing to joint opening,

666 and then vibrated which transforms the impact energy to kinetic energy of the column. The

667 deflection of the segmental column also led to the stretch of the prestress tendon. Localized

668 plastic deformation was observed on the prestress tendon around the mid-height of the

669 column. Therefore the plastic deformation of prestress tension would also dissipate energy.

670 Other means such as concrete crushing damage, friction between segments at joints etc.

671 would also dissipate impact energy.

672 **5. Summary**

673 In this paper, we performed pendulum impact tests to investigate the impact resistance

674 capacity of segmental columns. The fundamental behaviour of precast segmental column

675 with posttensioning tendon under impact force was studied. Comparison was made

676 between segmental column and conventional monolithic column. The deformation-to-

677 failure processes of the columns were monitored by a high-speed camera. The impact load

678 and the lateral displacement time histories were measured and used to evaluate column

679 performance. The testing results concluded that the segmental column is more flexible than

680 conventional monolithic column. Under high level impact, segmental joints near and above

681 the impacted segment would open. Column with more segmental joints is more flexible with

682 multiple openings at the joints near the impact location. Because of the relatively lower

683 stiffness of segmental columns, smaller peak impact forces but similar impact impulses were

684 measured on these columns as compared with those on monolithic column when the

685 impactor was striking at the same velocity. The segmental columns have better self-centring

686 capacity with smaller residual displacements as compared to the monolithic column. With

687 the same column dimension and reinforcement ratio, similar level of energy could be

688 dissipated by the segmental column and the monolithic column; but the segmental column

689   experienced relatively less damages with partial impact energy absorbed by other

690   mechanism such as joint opening, friction and more column vibration.

696   **Reference**

697   [1] M. Shahawy, Prefabricated Bridge Elements and Systems to limit traffic disruption during
698   construction, Technical Report, Transportation Research Board, 2003.
699   [2] M.M. Sprinkel, Prefabricated bridge elements and systems, NCHRP Synthesis of Highway
700   Practice, (1985).
701   [3] Y.-C. Ou, Precast segmental post-tensioned concrete bridge columns for seismic regions,
702   PhD thesis, State University of New York at Buffalo, 2007.
703   [4] S. Billington, R. Barnes, J. Breen, Alternate substructure systems for standard highway
704   bridges, Journal of Bridge Engineering, 6 (2001) 87-94.
705   [5] Y.-C. Ou, M. Chiewanichakorn, A.J. Aref, G.C. Lee, Seismic performance of segmental
706   precast unbonded posttensioned concrete bridge columns, Journal of structural engineering,
707   133 (2007) 1636-1647.
708   [6] C.S. Shim, C.-H. Chung, H.H. Kim, Experimental evaluation of seismic performance of
709   precast segmental bridge piers with a circular solid section, Engineering Structures, 30 (2008)
710   3782-3792.
711   [7] T.-H. Kim, H.-M. Lee, Y.-J. Kim, H. Shin, Performance assessment of precast concrete
712   segmental bridge columns with a shear resistant connecting structure, Engineering
713   Structures, 32 (2010) 1292-1303.
714   [8] M.A. ElGawady, H.M. Dawood, Analysis of segmental piers consisted of concrete filled
715   FRP tubes, Engineering Structures, 38 (2012) 142-152.
716   [9] H. Dawood, M. ElGawady, J. Hewes, Behavior of segmental precast posttensioned bridge
717   piers under lateral loads, Journal of Bridge Engineering, 17 (2011) 735-746.
718   [10] Z. Wang, J. Ge, H. Wei, Seismic performance of precast hollow bridge piers with
719   different construction details, Frontiers of Structural and Civil Engineering, 8 (2014) 399-413.
720   [11] E. Nikbakht, K. Rashid, F. Hejazi, S.A. Osman, Application of shape memory alloy bars in
721   self-centring precast segmental columns as seismic resistance, Structure and Infrastructure
722   Engineering, 11 (2015) 297-309.
723   [12] C.H. Chung, J. Lee, J.H. Gil, Structural performance evaluation of a precast prefabricated
724   bridge column under vehicle impact loading, Structure and Infrastructure Engineering, 10
725   (2014) 777-791.
726   [13] Y. Sha, H. Hao, Laboratory tests and numerical simulations of barge impact on circular
727   reinforced concrete piers, Engineering Structures, 46 (2013) 593-605.
728   [14] C.E. Buth, W.F. Williams, M.S. Brackin, D. Lord, S.R. Geedipally, A.Y. Abu-Odeh, Analysis
729   of large truck collisions with bridge piers: phase 1. Report of guidelines for designing bridge
730   piers and abutments for vehicle collisions, 2010.

731 [15] C.E. Buth, M.S. Brackin, W.F. Williams, G.T. Fry, Collision Loads on Bridge Piers: Phase 2.
732 Report of Guidelines for Designing Bridge Piers and Abutments for Vehicle Collisions, 2011.
733 [16] P.F. Silva, W.D. Mesia, D. Marzougui, S.S. Badie, Performance evaluation of flexure
734 impact resistance capacity of reinforced concrete members, ACI Structural Journal, 106
735 (2009).
736 [17] S. El-Tawil, E. Severino, P. Fonseca, Vehicle collision with bridge piers, Journal of Bridge
737 Engineering, 10 (2005) 345-353.
738 [18] S.C. Woodson, J.T. Baylot, Structural collapse: quarter-scale model experiments, DTIC
739 Document, available online, 1999.
740 [19] S.C. Woodson, J.T. Baylot, Quarter-scale building/column experiments, Adv. Technol.
741 Struct. Eng, (2000) 1-6.

742

743
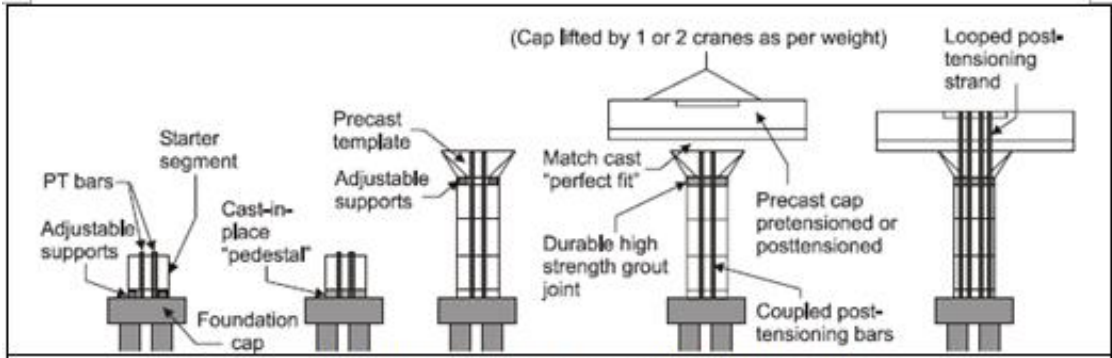
a) Erction sequence of a segmental column [4]

b) Brandenburg Gate, Germany, built in 1788-1791

c) Tempo in Rhodes island, Greece built around 7th Century B.C.

744

745 **Figure 1 Ancient and modern constructions of segmental columns**

746

| a) Monolithic column | b) Segmental column - S5N | c) Segmental column - S7N |
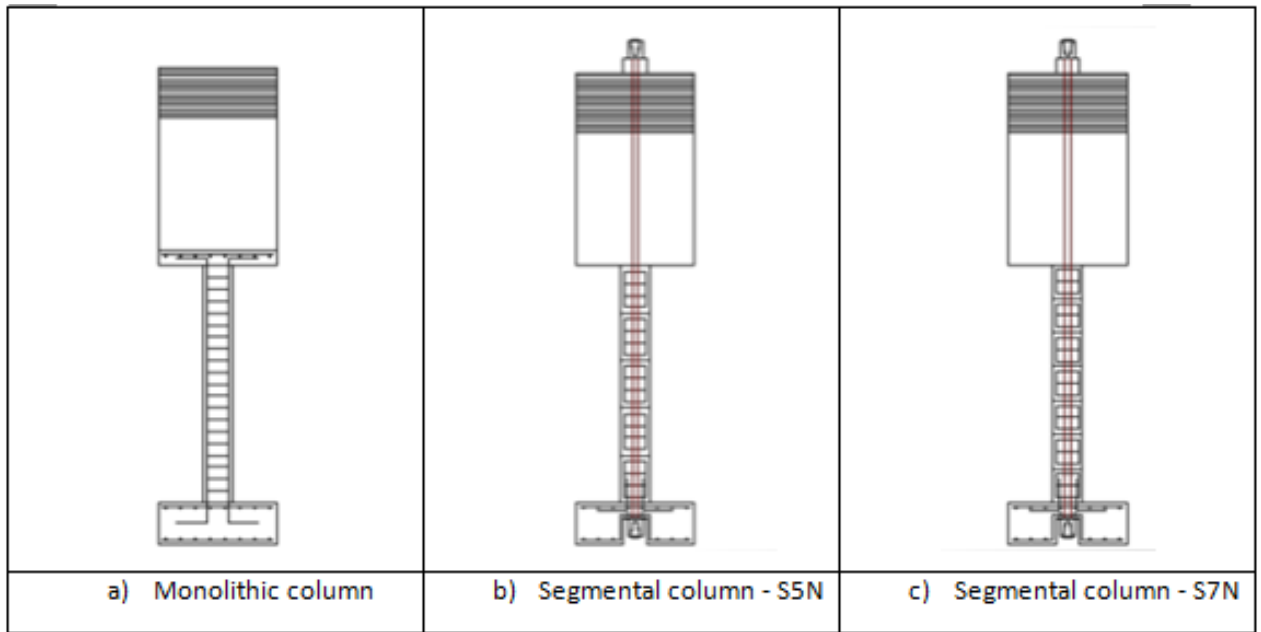
Figure 2 Schematic views of the test specimens
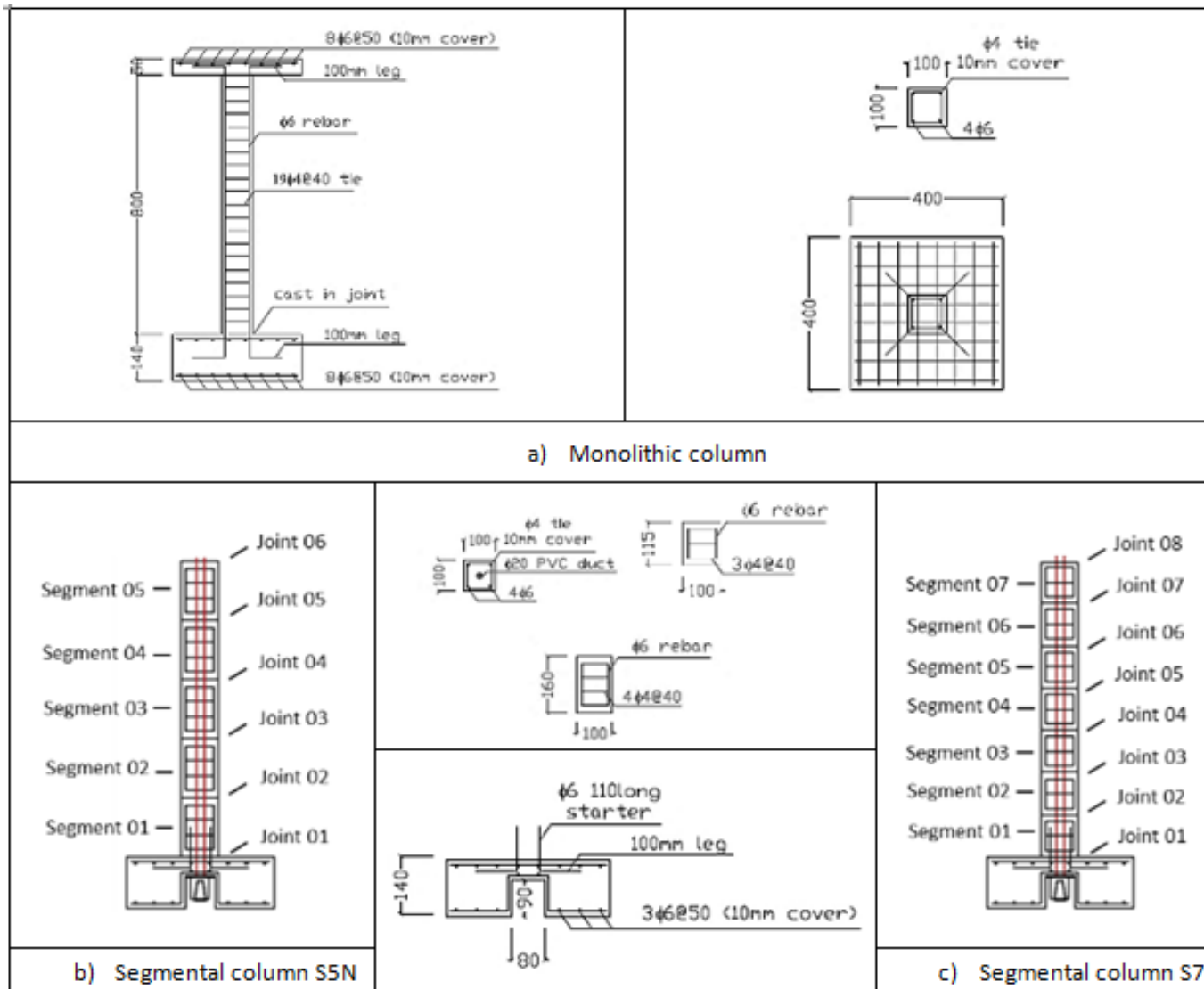
Figure 3 Details of the test specimens

a) Reinforcment cage for column S7N	b) Footing for segmental column

c) Formwork for monolithic column

d) Formwork for segmental columns and the casted column S5N

753
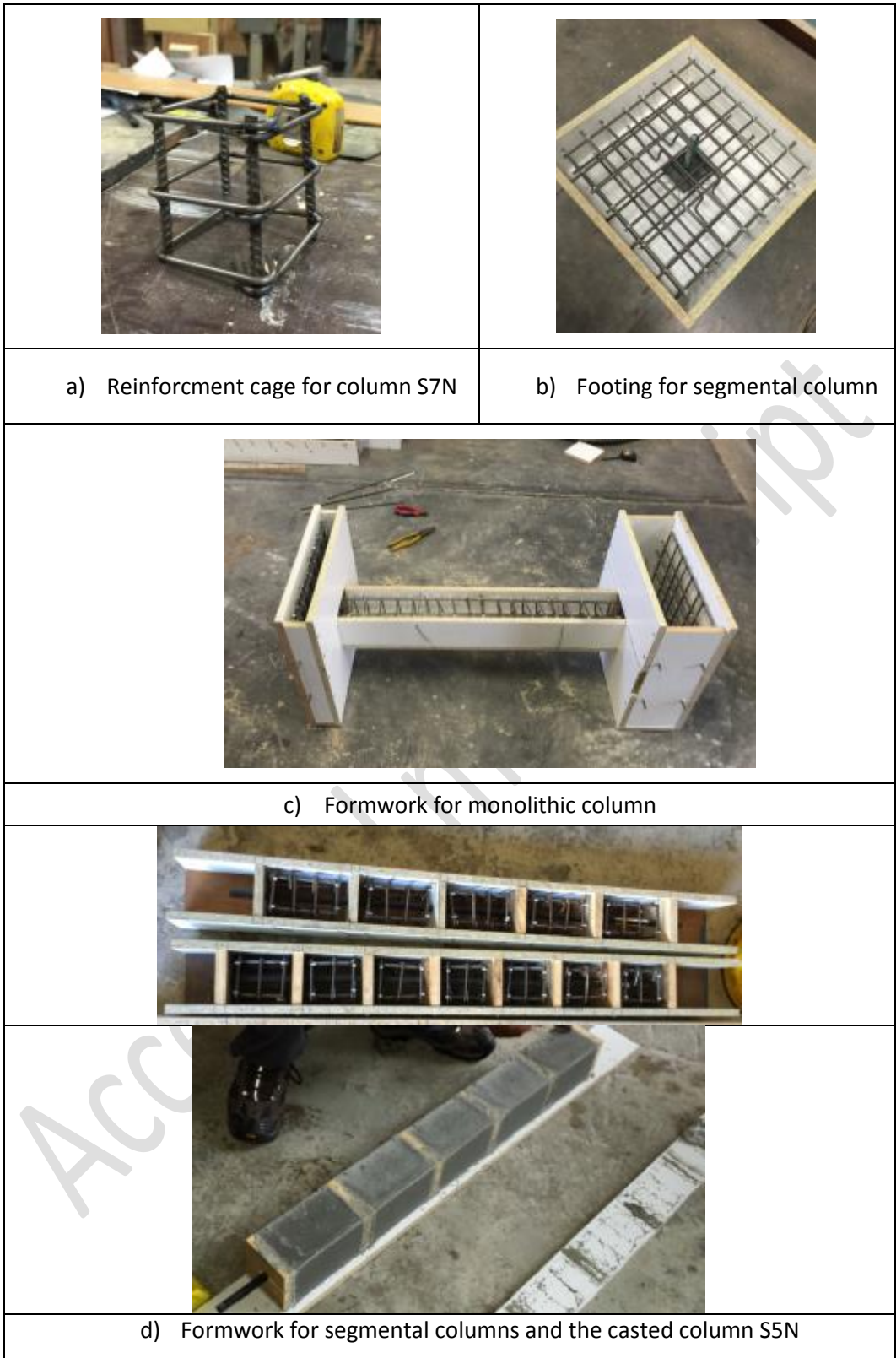
754
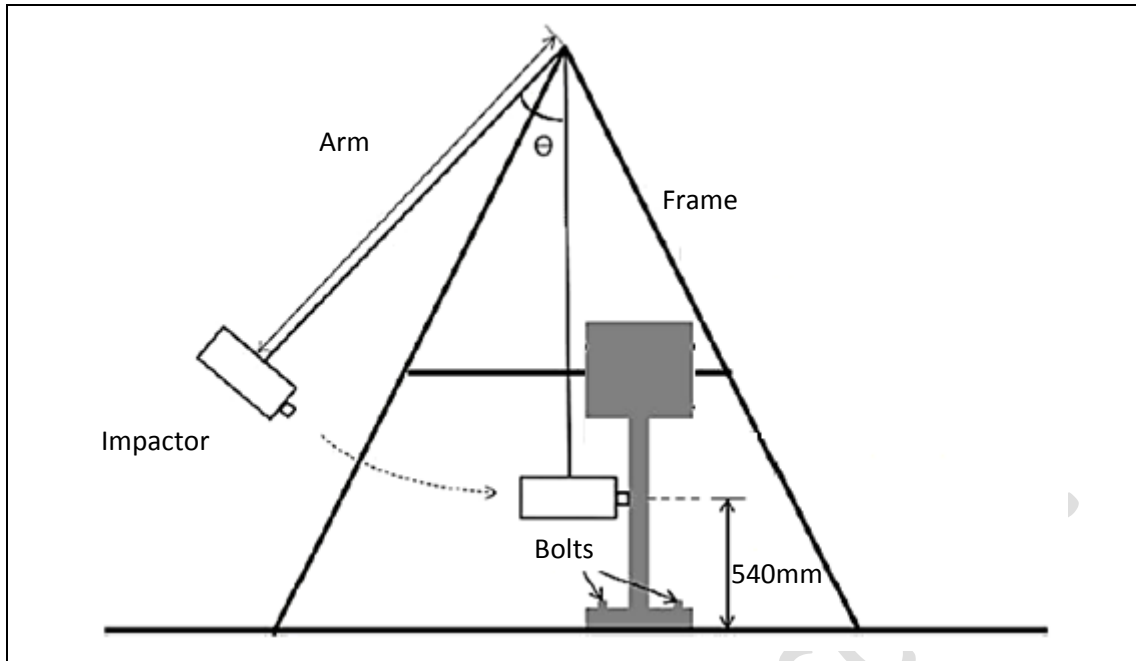
a) Schematic view of pendulum impact system

b) The ready-to-go impact system and setup details

Figure 5 Pendulum impact system and the test setup

757
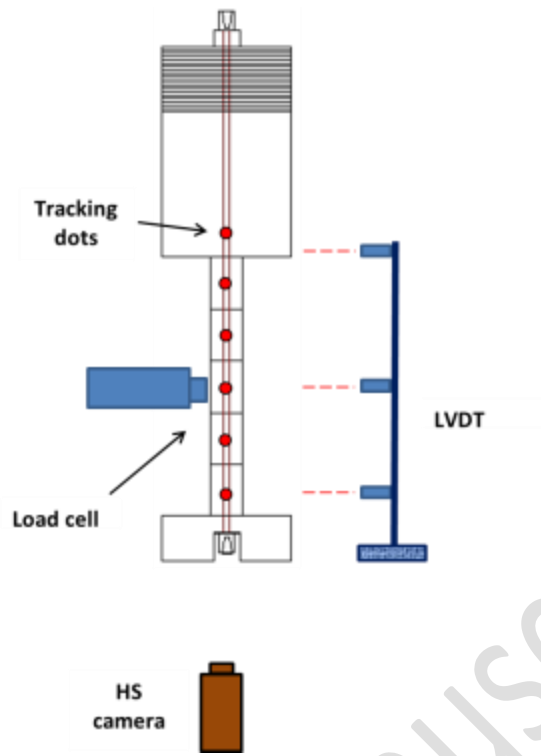
Figure 6 Measurement system for the pendulum impact test

759

Monolithic column

Segmental column S5N

Segmental column S7N
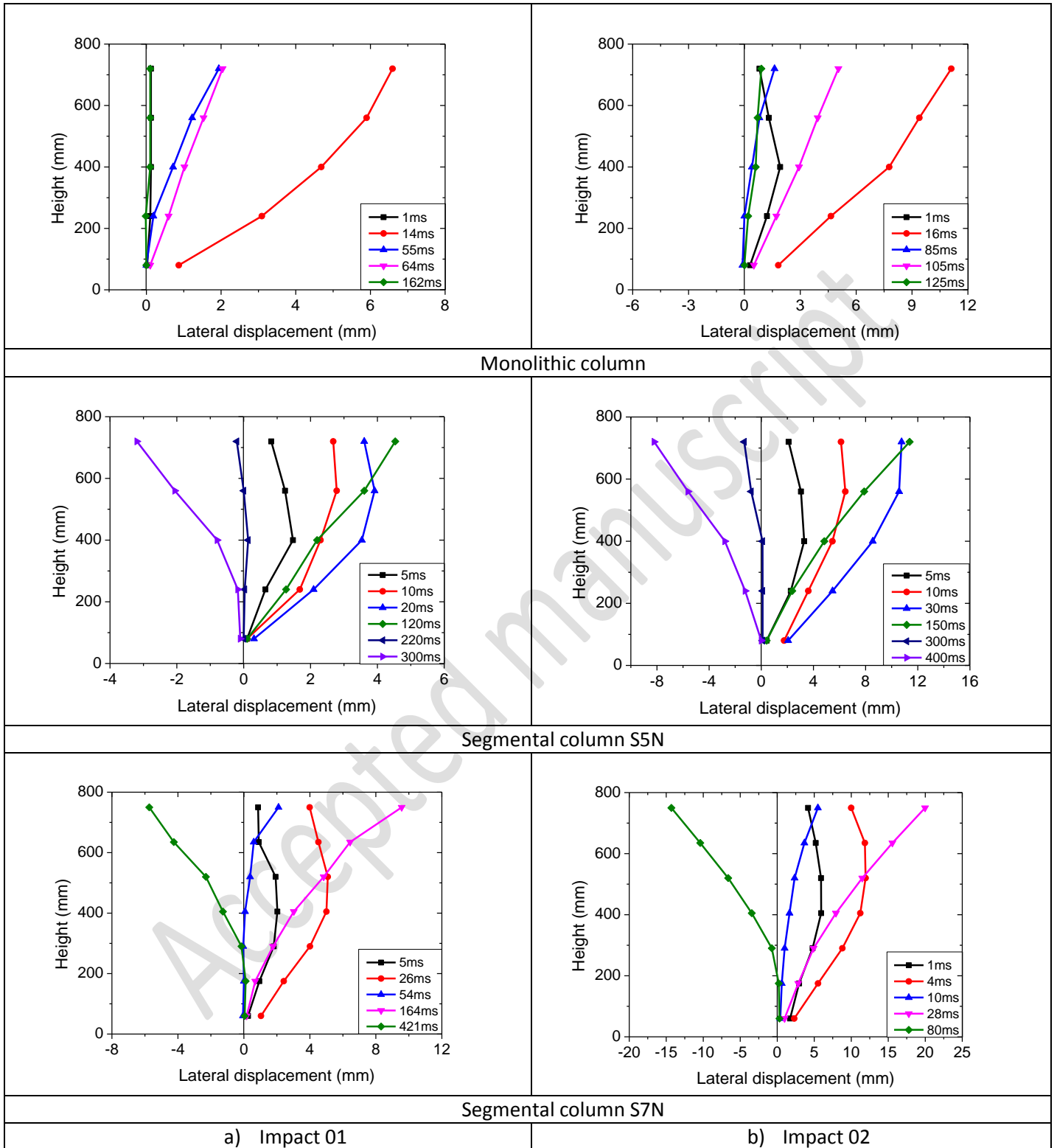
| a) Impact 01 | b) Impact 02 |

Figure 7 Column lateral displacement contours in Impact 01 and 02

t=0ms

t=0ms

t=0ms

t=5ms

t=5ms

t=1ms

t=26ms

t=45ms

t=6ms

t=55ms

t=98ms

t=13ms

t=66ms	t=252ms	t=37ms
t=124ms	t=676ms	t=110ms
a) Monolthic	b) Column S5N	c) Column S7N
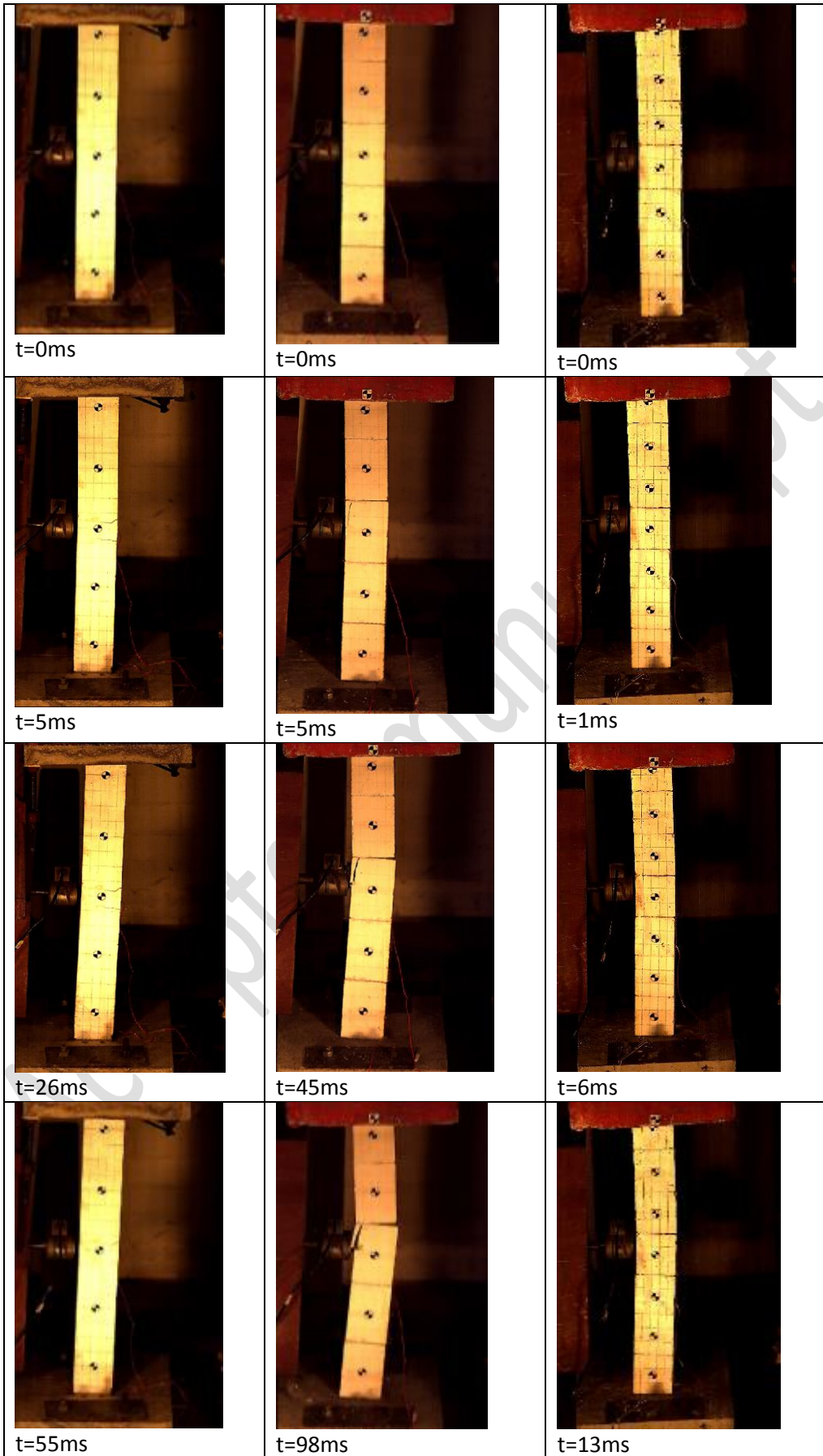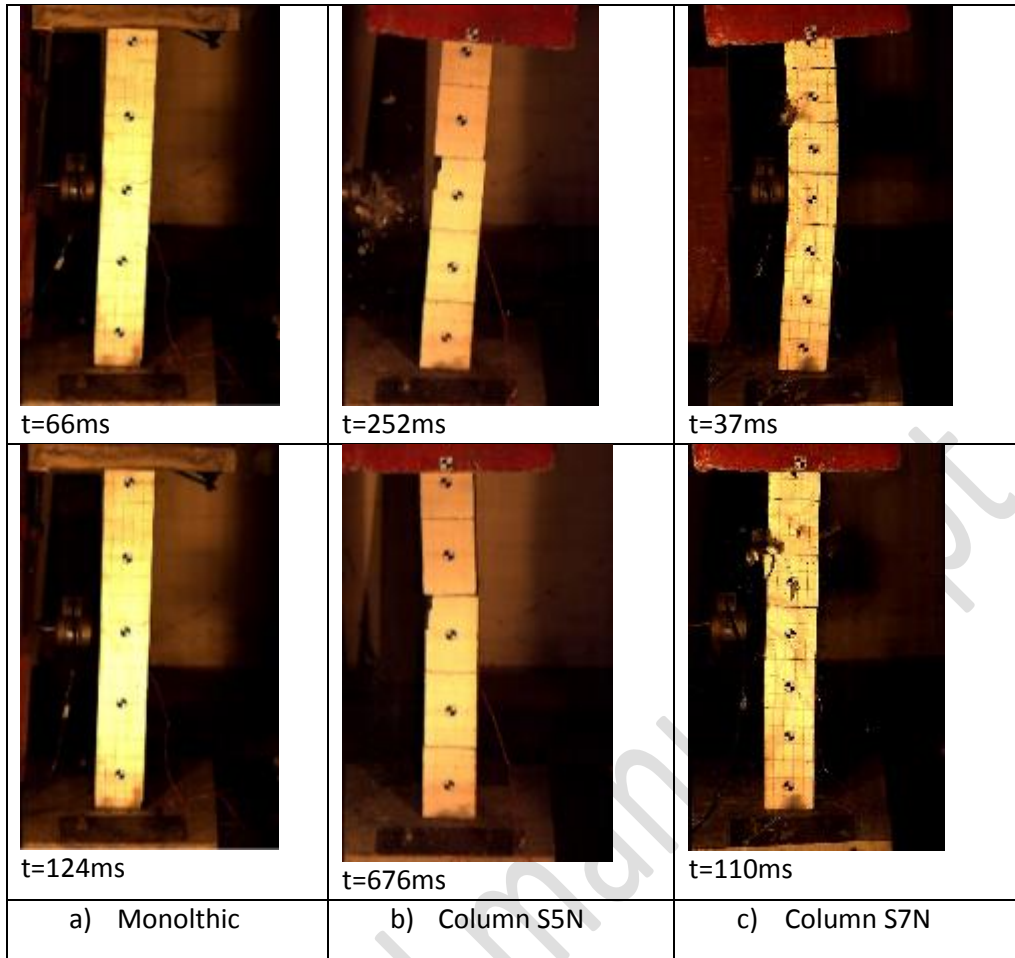
763   **Figure 8 High-speed camera images of columns in Impact 03**

764

t=0ms	t=0ms	t=0ms	t=0ms
t=0.4ms	t=5ms	t=5ms	t=5ms
t=4ms	t=78ms	t=120ms	t=75ms
t=7ms	t=199ms	t=221ms	t=213ms

t=57ms	t=425ms	t=400ms	t=313ms
t=139ms	t=1250ms	t=1230ms	t=893ms
a) Monolithic (Impact 04)	b) S5N (Impact 04)	c) S7N (Impact 04)	d) S7N (Impact 05)

765

766
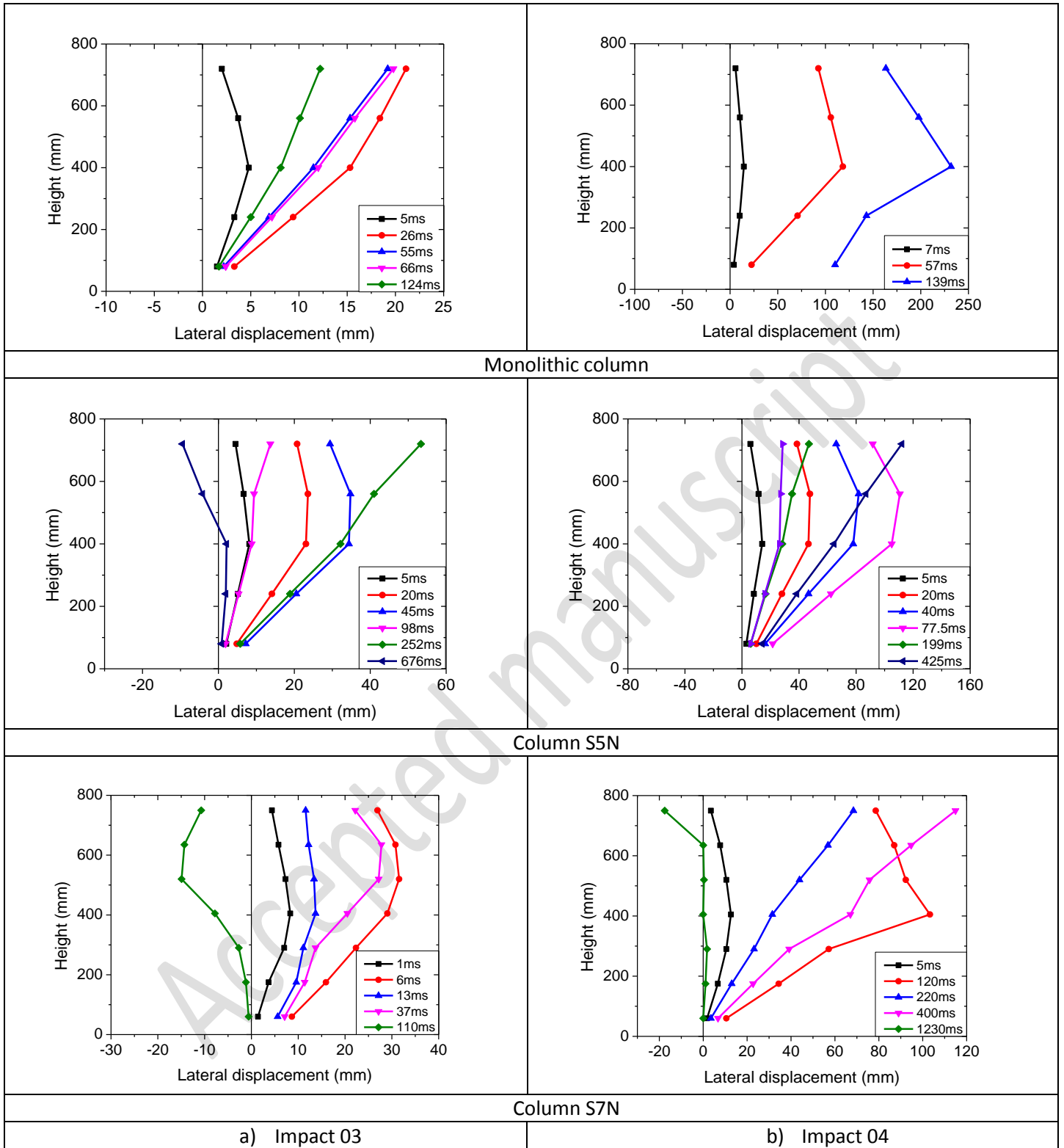
Figure 10 Column displacement histories and displacement contours in Impact 03 and 04
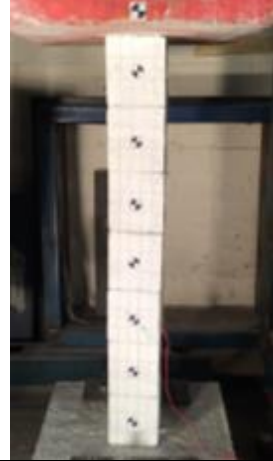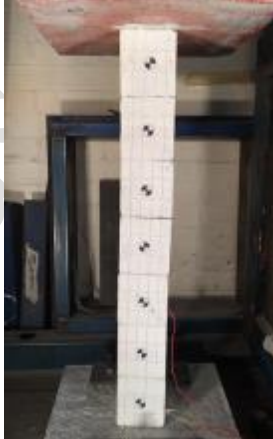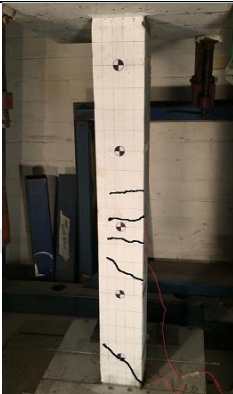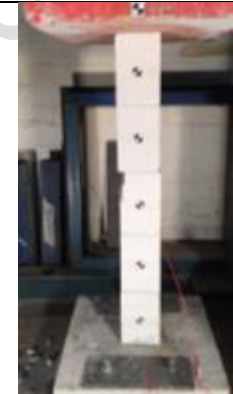
| Monolithic | Column S5N | Column S7N |

a) Post-impact status of columns after Impact 01

| Monolithic | Column S5N | Column S7N |

b) Damage to columns after Impact 02

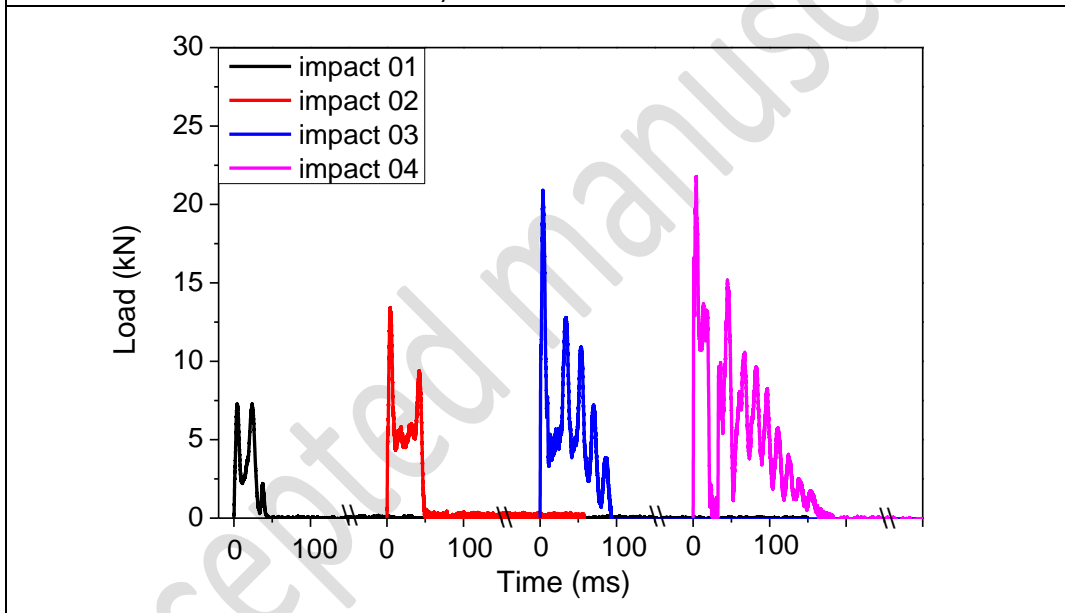| Monolithic | Column S5N | Column S7N |

c) Damage to columns after Impact 03

Monolithic	Column S5N	Column S7N
d) Damage to columns after Impact 04		

e) Damage to column S7N after Impact 05

Figure 11 Post-impact status of columns
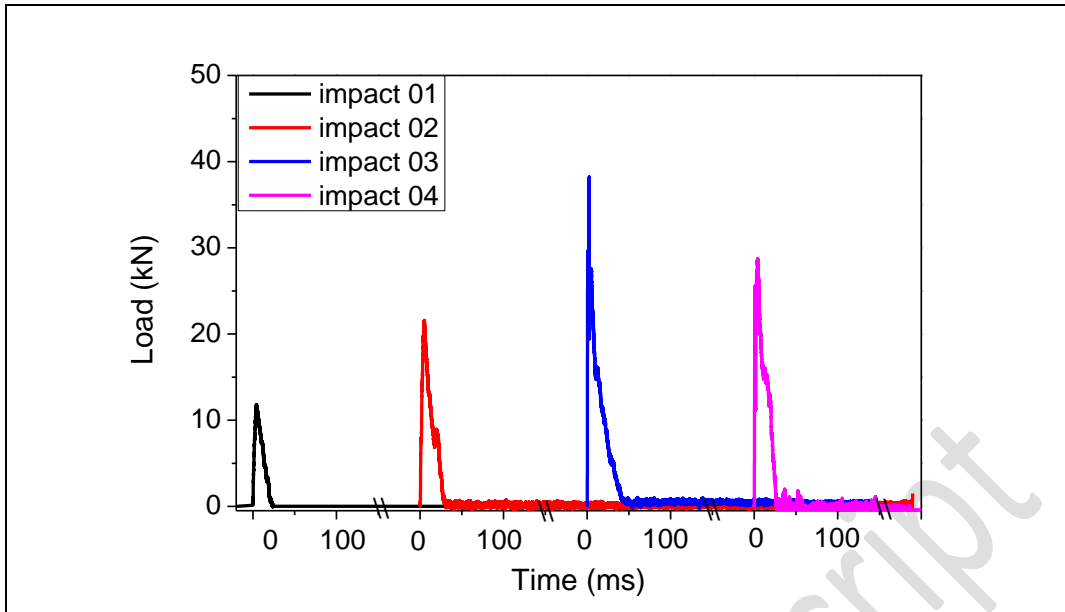
a)   Monolithic column

b)   Segmental column S5N
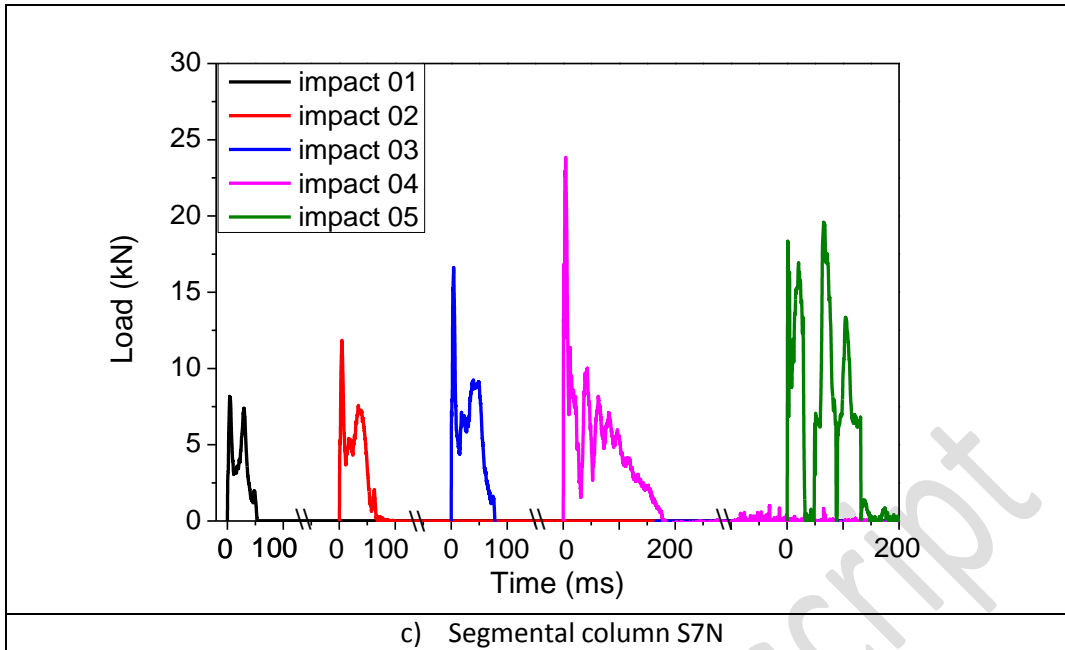
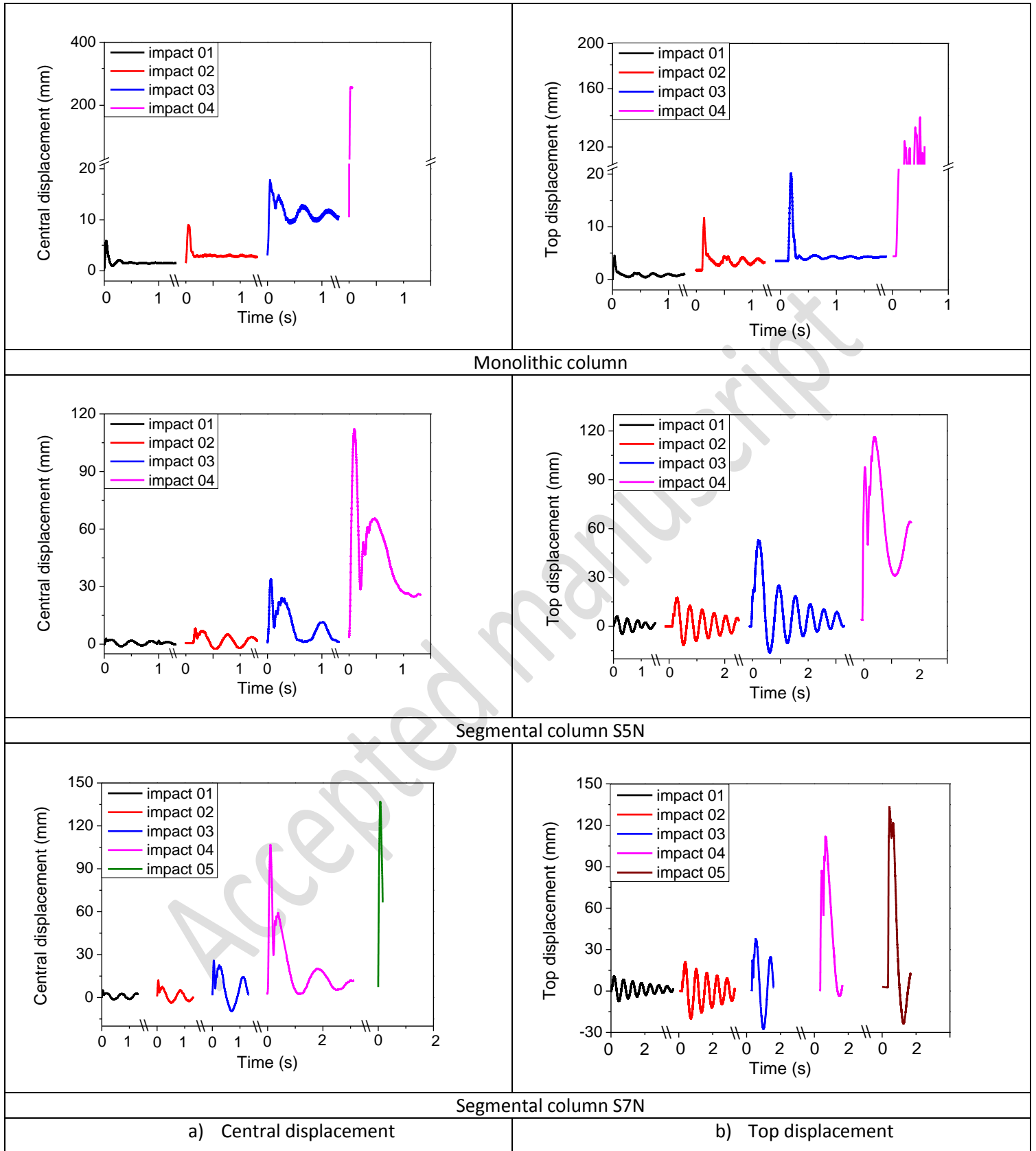c) Segmental column S7N

Figure 12 Load time histories
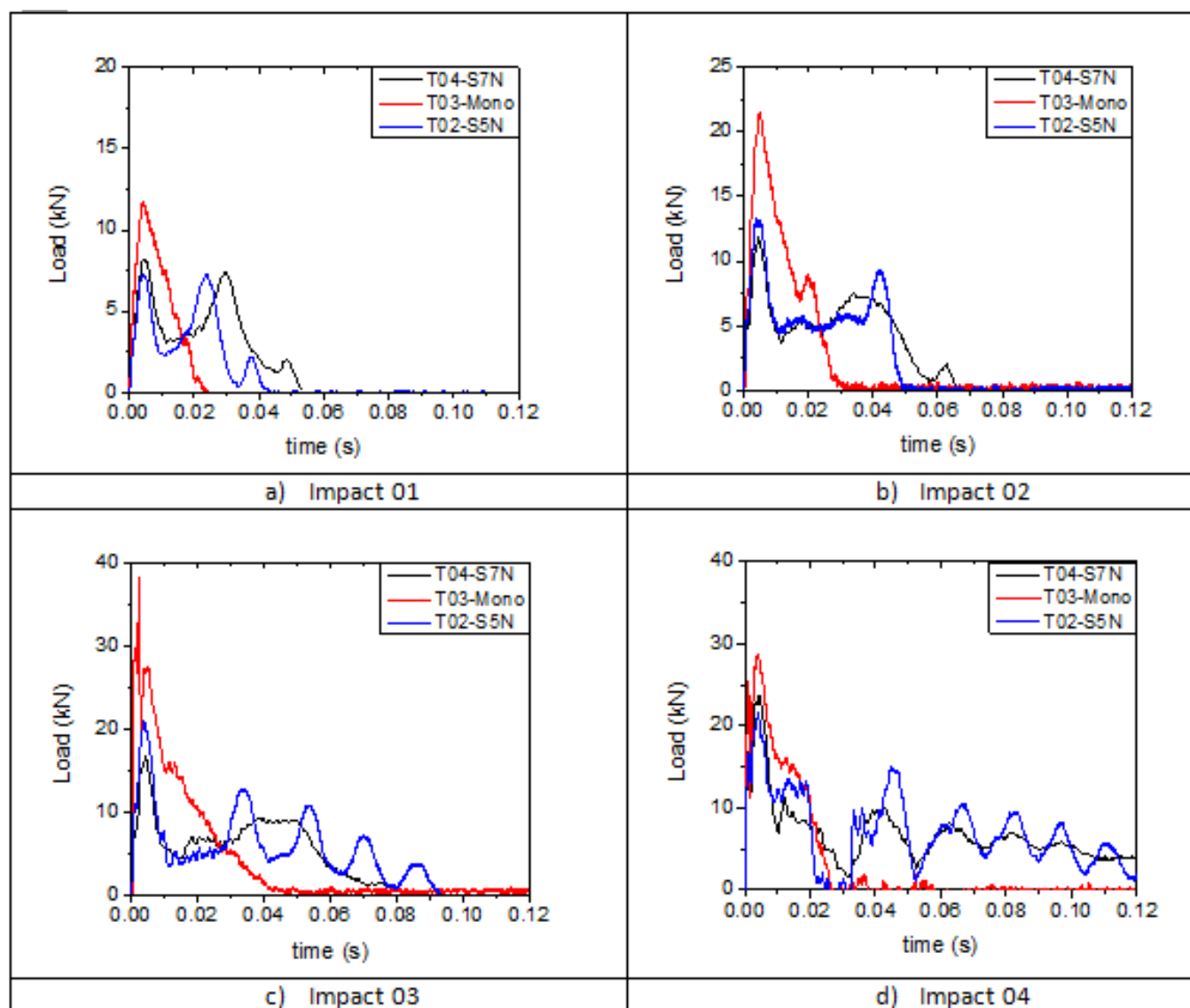
Monolithic column

Segmental column S5N

Segmental column S7N

| a) Central displacement | b) Top displacement |

Figure 13 Column central and top lateral displacement time histories

a) Impact 01

b) Impact 02

c) Impact 03

d) Impact 04

Figure 14 Comparison of load time histories
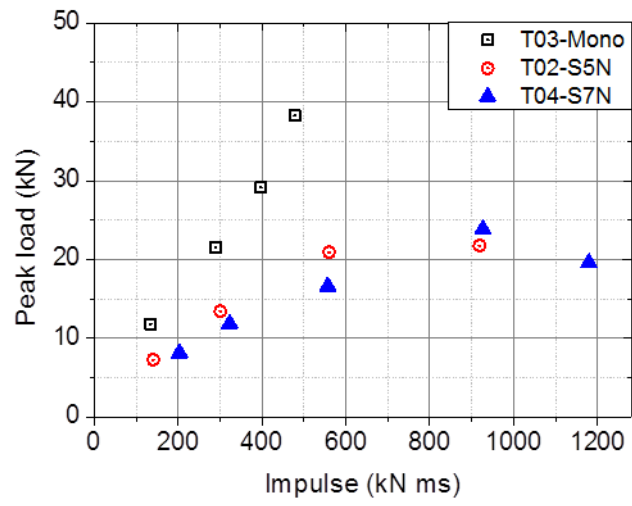
778

779

780

a) Impact 01

b) Impact 02

c) Impact 03

d) Impact 04
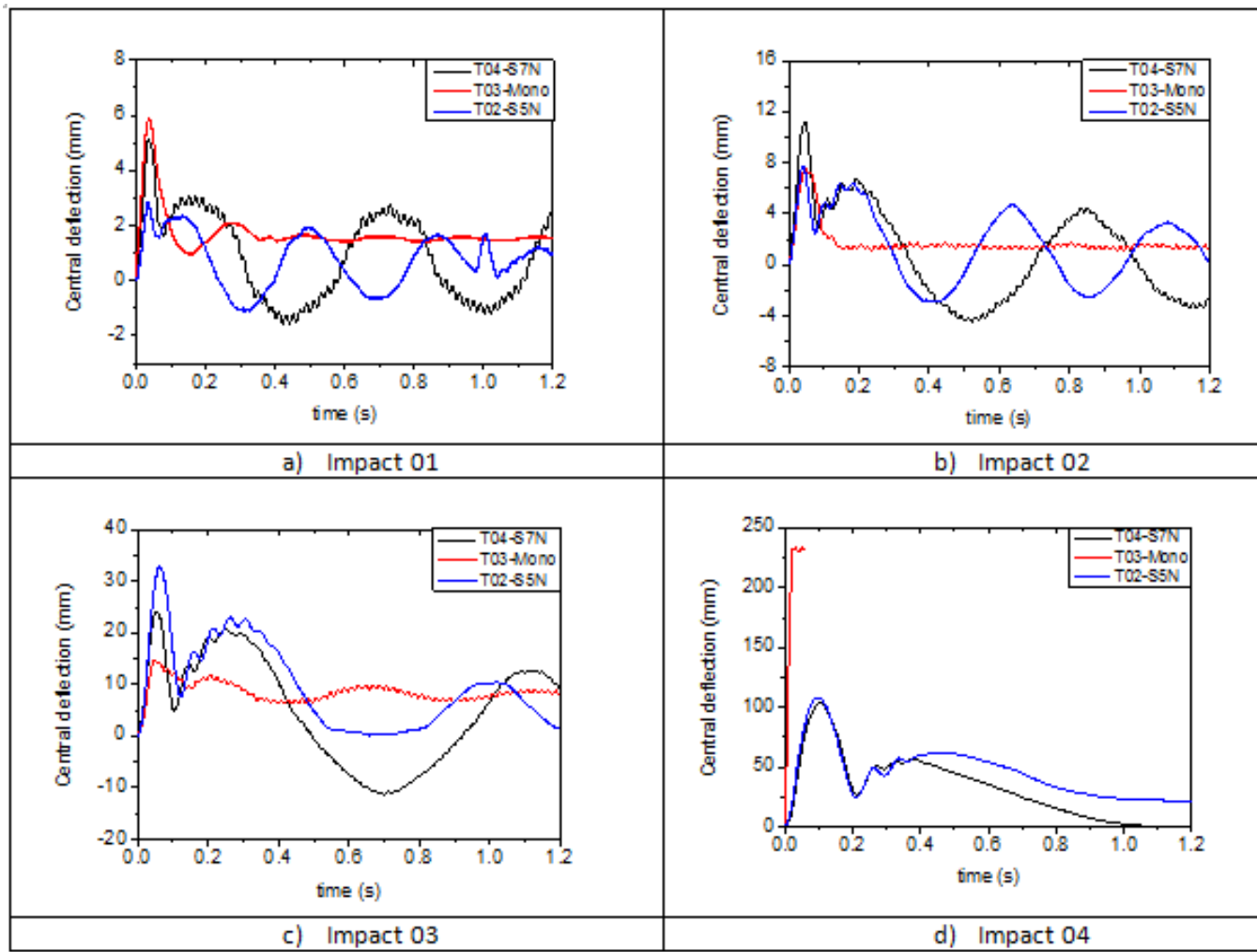
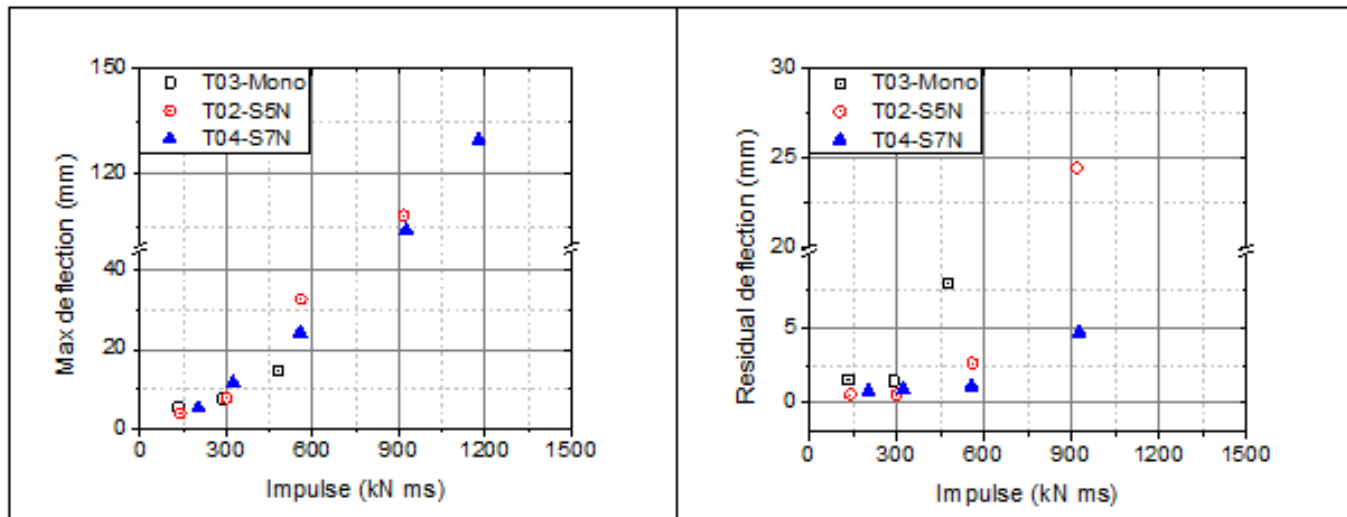**Figure 16 Comparison of column central deflection time histories**

49

784

785   Figure 17 Maximum central deflection and residual deflection versus impulse

786

787

788

789

51
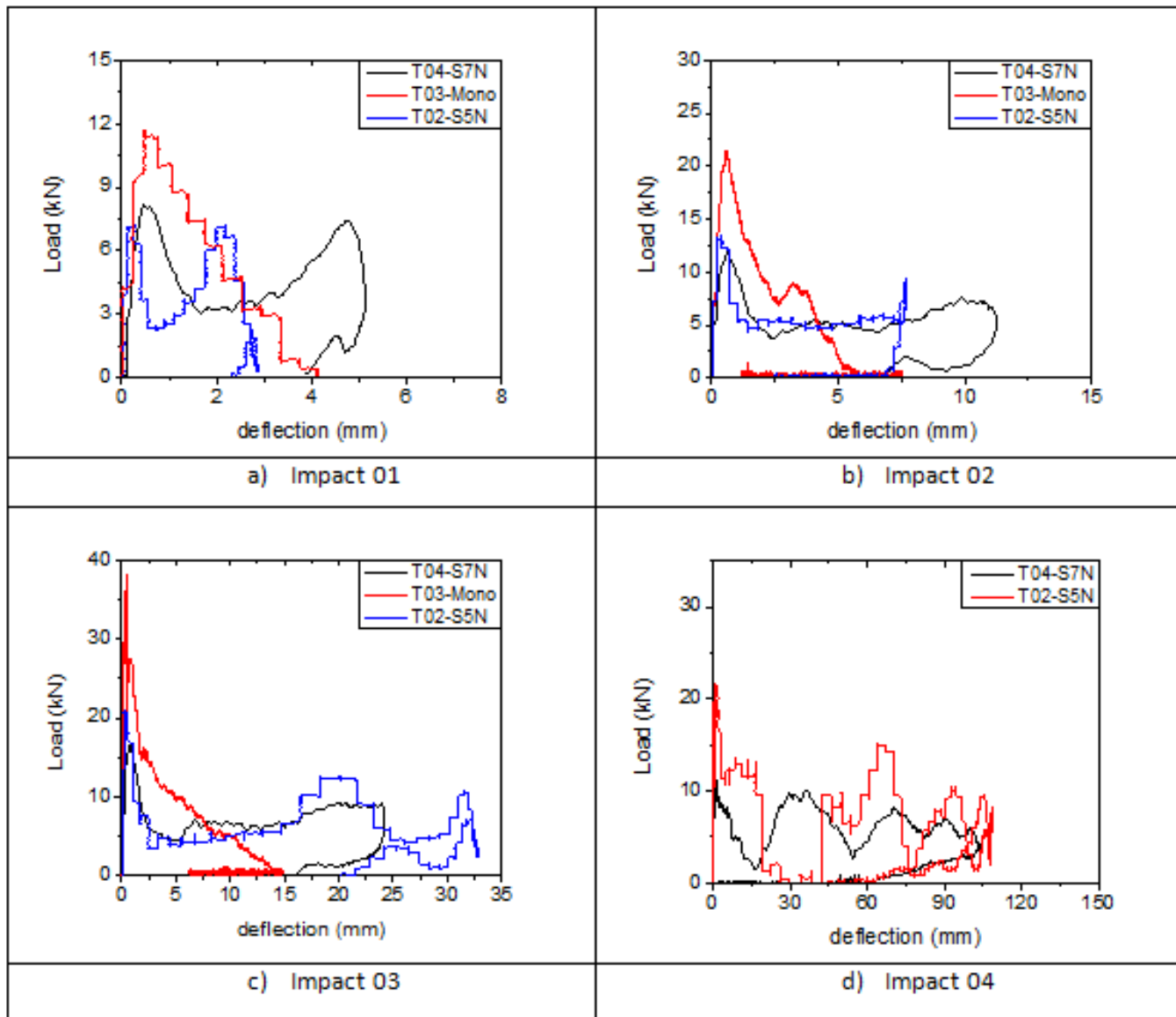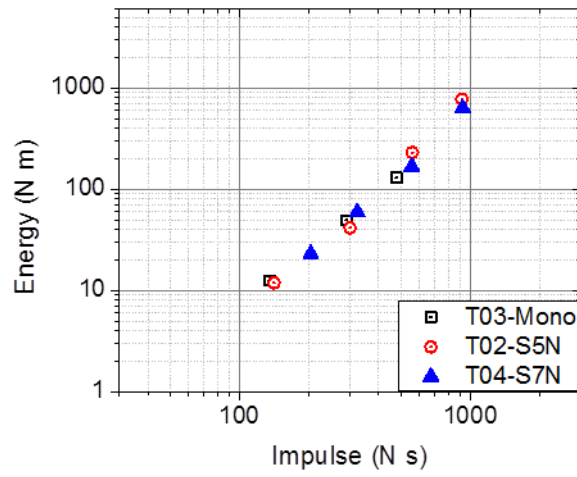
790

791   **Figure 19 Energy dissipation vs impulse**

792

Column	Height (mm)	Cross-section dimension (mmxmm)	$\phi_{long, rebar}$* (mm)	ϕ_{tie}* (mm)	Longitudinal reinforcement ratio (%)
Monolithic	800	100 x 100	6	4	1.14
S5N	800	100 x 100	6	4	1.16
S7N	800	100 x 100	6	4	1.16

793   * φ stands for the diameter of reinforcement
794   **Table 1 Specifications of the test specimens**

795

Material	ρ (kg/m3)	fc' (MPa)	f_t, f_y (or f_{proof}) (MPa)	E (GPa)
Concrete	2400	34	5	30
Longitudinal rebar	7800	-	500	200
Tie	7800	-	300	200
Prestress tendon	7850	-	1860	195

796

Table 2 Material properties

797

Specimen	Impact 01		Impact 02		Impact 03		Impact 04		Impact 05	
	F_{peak} (kN)	I (kN ms)	F_{peak} (kN)	I (kN ms)	F_{peak} (kN)	I (kN ms)	F_{peak} (kN)	I (kN ms)	F_{peak} (kN)	I (kN ms)
Monolithic	11.81	134	21.58	290	38.22	478	29.12	397	-	-
S5N	7.29	141	13.44	301	20.91	560	21.78	918	-	-
S7N	8.17	203	11.85	323	16.61	557	23.85	926	19.59	1179

798 **Table 3 Summary of impact loads**

799

Specimen	Impact 01		Impact 02		Impact 03		Impact 04		Impact 05	
	F_{peak} (kN)	I (kN ms)	F_{peak} (kN)	I (kN ms)	F_{peak} (kN)	I (kN ms)	F_{peak} (kN)	I (kN ms)	F_{peak} (kN)	I (kN ms)

800   a) Column central maximum and residual displacements

Specimen	Impact 01		Impact 02		Impact 03		Impact 04	
	δ_{max} (mm)	$\delta_{resi.}$ (mm)	δ_{max} (mm)	$\delta_{resi.}$ (mm)	$\delta_{resi.}$ (mm)	δ_{max} (mm)	δ_{max} (mm)	$\delta_{resi.}$ (mm)
Monolithic	5.2	1.5	7.5	2.9	14.6	11.0	-	-
S5N	3.0	0.5	7.7	1.0	32.8	3.6	108.4	28.0
S7N	5.1	0.7	11.5	1.6	24.3	2.6	104.2	7.3

801   * δ represents lateral displacement

802   b) Column top maximum and residual displacements

Specimen	Impact 01		Impact 02		Impact 03		Impact 04	
	δ_{max} (mm)	$\delta_{resi.}$ (mm)	δ_{max} (mm)	$\delta_{resi.}$ (mm)	δ_{max} (mm)	$\delta_{resi.}$ (mm)	δ_{max} (mm)	$\delta_{resi.}$ (mm)
Monolithic	6.6	1.9	11.7	3.7	21.1	4.3	-	-
S5N	6.1	0.7	17.6	1.8	52.9	3.8	116.3	41.8
S7N	10.6	0.7	21.0	2.4	37.6	4.4	111.9	6.9

803   * δ represents lateral displacement
804   **Table 4 Summary of maximum and residual displacements**

805

806